STEAM GENERATOR TUBE RUPTURE STUDY

Final Report

by

S. T. Free

A. L. Schor

Massachusetts Institute of Technology
Department of Nuclear Engineering
and
Energy Laboratory
Cambridge, Massachusetts 02139

MIT-EL 86-006

May 1986

STEAM GENERATOR TUBE RUPTURE STUDY

by

S. T. Free and A. L. Schor

ABSTRACT

This report describes our investigation of steam generator behavior during a postulated tube rupture accident. Our study was performed using the steam generator, thermal-hydraulic analysis code THERMIT-UTSG. The purpose of our work was to provide an independent assessment of the Los Alamos National Laboratory system code TRAC-PF1 with respect to steam generator tube rupture analysis. Results of our work are presented and compared with previous TRAC-PF1 results. There are substantial differences in the results of the two codes. These discrepancies are discussed and deficiencies in both codes are noted. Our results lead us to believe that further investigation and code development are necessary to gain more than a basic understanding of steam generator behavior during such accidents and to provide a simulation capability that is acceptable.

Acknowledgements

We would like to recognize the Los Alamos National Laboratory for funding this project and allowing the use of their computing facility. We express our appreciation to Messrs. Bahran Nassersharif and John Ireland of the Safety Analysis Code Development Group, for their technical assistance and encouragement. We extend our thanks also to Dr. Hugo da Silva of Yankee Atomic Electric Company, author of THERMIT-UTSG, for his helpful advice throughout this project.

Table of Contents

List of Figures

List of Tables

Steam Generator Tube Rupture Study

I. Introduction

Steam generator tube rupture (SGTR) transients have recently received attention because of their frequency of occurrence and potential severity. There have been several SGTR events at such operating pressurized water reactors as Ginna, Point Beach Unit 1, Surry Unit 2, and Prairie Island Unit 1. An SGTR event represents a breach of the primary system. Hence, there is an obvious concern about the amount and rate of radioactive material release. Some existing Final Safety Analysis Reports (FSAR) have stated that the leakage from the primary to the secondary system due to a SGTR can be terminated in 30 minutes and overfilling of the damaged steam generator does not occur. However, during actual plant accidents the leakage has continued for several hours and overfill has occurred. Therefore, a reexamination of this safety issue is needed.

This report describes the work that has been done in support of the SGTR analyses performed at the Los Alamos National Laboratory (LANL) for the Nuclear Regulatory Commission. The LANL study deals with the overall system response to several postulated SGTR accident scenarios, focusing on the particular SGTR event that is thought to have the greatest potential for the largest release of radioactive material to the environment -- a double-ended rupture of a single steam generator tube. Their study used TRAC-PF1, a thermal-hydraulic system code, to simulate the behavior of the Calvert Cliffs Nuclear Plant during such types of SGTR transients. The results of the LANL work as of this time are reported in Reference [1].

Our role in this study was to provide an independent assessment of some of the TRAC calculations. For this work we have used the recently developed MIT code THERMIT-UTSG [2]. This code simulates the thermal-hydraulic behavior of a U-tube steam generator under transient conditions. Modifications were made to include the leakage flow into the secondary side from a SGTR.

In this report we present the results of our calculations with THERMIT-UTSG and compare them with the TRAC results. First, we give a brief description of the code, followed by a description of the Calvert Cliffs steam generator model. Next, we show the results of our steady-state calculation. This is followed by a presentation of the work that was done to assess the impact of the different THERMIT and TRAC heat transfer correlations on the results. We then show the results of the transient calculations performed in our analysis. The final section summarizes our findings and conclusions.

II. THERMIT-UTSG

THERMIT-UTSG [2] is a dynamic, thermal-hydraulic model of a U-tube steam generator (UTSG). It was developed by specializing the two-fluid, multi-dimensional code THERMIT2 [3] for steam generator component analysis and coupling it to a recirculation model, representing the dynamics of the steam separators/dryers, steam dome, and upper downcomer. In this section we first describe THERMIT2, as it is the foundation for the steam generator model. Then, we discuss how it was adapted for steam generator component simulation.

II.1 THERMIT-2

THERMIT2 is an improved version of the original THERMIT code [4], developed at MIT in 1977-78, under EPRI sponsorship.

THERMIT employs a full six-equation ("two-fluid"), two-phase flow model in a three-dimensional, Cartesian geometry configuration. Its original constitutive relation package was tailored to a reactor core-wide analysis. The newer version, THERMIT2, contains an upgraded package, including provisions for interchannel turbulent exchanges, which make it suitable for subchannel-type analysis as well. The presence of solids in the flow field is handled by providing actual fluid volumes and flow areas, which may not be equivalent to their corresponding geometric counterparts.

The numerical scheme used by the code is a judicious compromise between implicit and explicit treatments. Short time-constant phenomena (sonic propagation and local interfacial couplings) are treated implicitly, while convection is accounted for explicitly. Formally, the stability limitation of the linearized problem is the convective time step, which for highly subsonic flows is obviously much more lenient

than the traditional Courant time-step. In many applications this semi-implicit treatment has been proven to be a reasonable approach in as far as the computational effort is concerned. Newton's method is used to solve the large set of non-linear equations. The particular temporal and spatial discretization allows the reduction of the linearized problem to a pressure-field solution. This feature is crucial to the numerical efficiency of the method, especially in multidimensional applications. The iterations are continued until mass residuals fall below an acceptable criterion.

An extensive experience has been accumulated with the code. The formulation and the solution method have both been proven to be a solid framework for further development and application.

II.2 U-Tube Steam Generator Modeling

A schematic diagram of a U-tube steam generator is shown in Figure 2-1. For modeling purposes we consider such a steam generator to consist of the following regions: primary side (primary fluid and metal of the U-tubes), evaporator, riser, steam dome, and downcomer.* Theoretically, THERMIT2 would be capable of representing all of these regions provided the local correlations for interphase and structural interactions are known. Such a model would of necessity be geometrically complex and computationally expensive. Since relatively little is known of the local behavior inside the steam dome, particularly within the steam separators, such an approach would probably not be useful.

---

*Strictly speaking, the evaporator is the region containing the U-tube bundle, and the riser is the flared section between the evaporator and the steam separators. Some of the literature does not distinguish between these regions, calling the entire region from the tube sheet to the steam separators the "riser".

THERMIT-UTSG divides the steam generator into three computational domains: two-fluid model (downcomer, evaporator, riser), recirculation model (steam dome and upper downcomer), and primary-side model. The mathematical representation of each domain is distinct from the others. Each model is then coupled explicitly to the others, and the entire steam generator model is driven by system boundary conditions supplied by the user.

The evaporator, riser, and downcomer regions are represented by the THERMIT2 two-fluid model. Because of symmetry, only half of the steam generator is modeled. A typical cross-section is shown in Figure 2-2. Four channels are used to represent the downcomer and two evaporator/riser channels are used -- one containing the hot side of U-tubes and the other containing the cold side. The downcomer channels communicate with the evaporator/riser only at the bottom (see Figure 2-3). Here, a zero flow boundary condition forces the downcomer flow up into the evaporator/riser. Currently, the code also prevents communication between the four downcomer channels so that there is no crossflow between them. The hot and cold evaporator/riser channels are in communication along their entire length.

The volume occupied by structural materials is inaccessible to flow. This includes the U-tubes in the evaporator. The user is responsible for providing flow areas and volumes consistent with the porous body formulation of THERMIT2. The user also defines the axial nodalization of this domain.

The two-fluid model is coupled to the primary-side model through the local wall temperature on the secondary-side of the U-tubes. It is also coupled to the recirculation model though the pressures p_d and

p_r at the top of the downcomer and riser, respectively. It should be noted that the mesh cells in the downcomer between the feedwater ring and the top of the domain (or the vapor-liquid interface and the top when the water level is below the feedwater ring) are included in both the two-fluid and recirculation model domains. In the two-fluid model they function as fictitious cells filled with water with a downcomer pressure at the top such that the flow rate is correct and having the enthalpy resulting from the mixing of the recirculation and feedwater streams. The mixing of these streams and accounting for the correct downcomer water volume and level are handled by the recirculation model.

The steam dome (including the separators/dryers) and the downcomer section above the feedwater ring or the liquid level, whichever is lower, are represented in the recirculation model. The primary functions of this model are to: calculate the outlet steam flow, set the pressures at the top of the riser and downcomer for the two-fluid model, track the mass of vapor and liquid within its domain, calculate the recirculation flow, mix the recirculation and feedwater flows, and calculte the water level in the downcomer. Two lumped parameter regions representing the vapor and liquid are used. Equations for the conservation of mass and energy are solved for each region. Flashing and condensation are properly accounted for through the restriction that the two phases are always in thermodynamic equilibrium. No momentum equations are used for these volumes. Instead, the following pressure drop relation is used:

$$p_r = p + \Delta p_{sep}$$

where: p_r = pressure at the top of the riser

p = pressure of the vapor in the steam dome

Δp_{sep} = pressure drop across the separators/dryers. It is determined from a correlation given by Burley [5].

The steam dome pressure is either given by the user as a system boundary condition or, alternatively, can be calculated from the outlet steam flow specified by the user. The pressure at the top of the downcomer is set to give the correct recirculation plus feedwater flow into the downcomer.

The primary-side model accounts for the heat lost from the primary coolant as it transits the U-tubes and the heat transfer across the tube walls. Different U-tubes have different lengths depending on the axial elevation of the bend. U-tubes which bend within a particular axial level as specified by the two-fluid model domain nodalization are grouped together into one representative tube, called a "tube bank". For each tube bank at every axial level the model calculates the temperatures of the primary fluid, primary-side wall surface, intermediate wall metal, and secondary-side wall surface. The secondary-side wall temperature distribution is then used to calculate the wall-to-fluid heat transfer in the two-fluid model. Fouling of the U-tubes due to crud deposition, tube wall thinning, or any other factor which may contribute to uncertainty in the model is accounted for as a change in the thermal conductivity of the U-tube metal. The primary coolant mass flow is split among the different tube banks based on the assumption of equal frictional pressure drop for all tubes between the inlet and outlet plena.

Time-dependent, system boundary conditions are required to drive the UTSG model. These are given in Table 2-1. Note that the downcomer

TABLE 2-1

System Boundary Conditions for THERMIT-UTSG

Steady-State	Transient
1. Primary Inlet Temperature	1. Primary Inlet Temperature
2. Primary System Pressure	2. Primary System Pressure
3. Power Level	3. Average Primary Mass Flux
4. Steam Dome Pressure	4. Steam Dome Pressure (or Outlet Steam Flow)
5. Feedwater Temperature	5. Feedwater Temperature
6. Water Level	6. Feedwater Flow Rate

water level and power are specified for a steady-state calculation, whereas they are calculated in a transient. Likewise, the average primary mass flux and the feedwater flow rate are specified for a transient but calculated at steady-state. The feedwater flow (as well as the outlet steam flow) at steady-state is determined by the power level according to the following relation:

$$W_f = W_s = \frac{\dot{Q}}{h_s - h_f}$$

where: W_f = feedwater flow rate

W_s = outlet steam flow rate

$\dot{Q}$ = power

h_s = outlet steam enthalpy (assumed to be the saturated vapor enthalpy at the steam dome pressure)

h_f = feedwater enthalpy

The primary mass flux is also determined at steady-state from the given power and primary inlet temperature (and the flow area). In addition to these boundary conditions the user must supply a fouling coefficient.

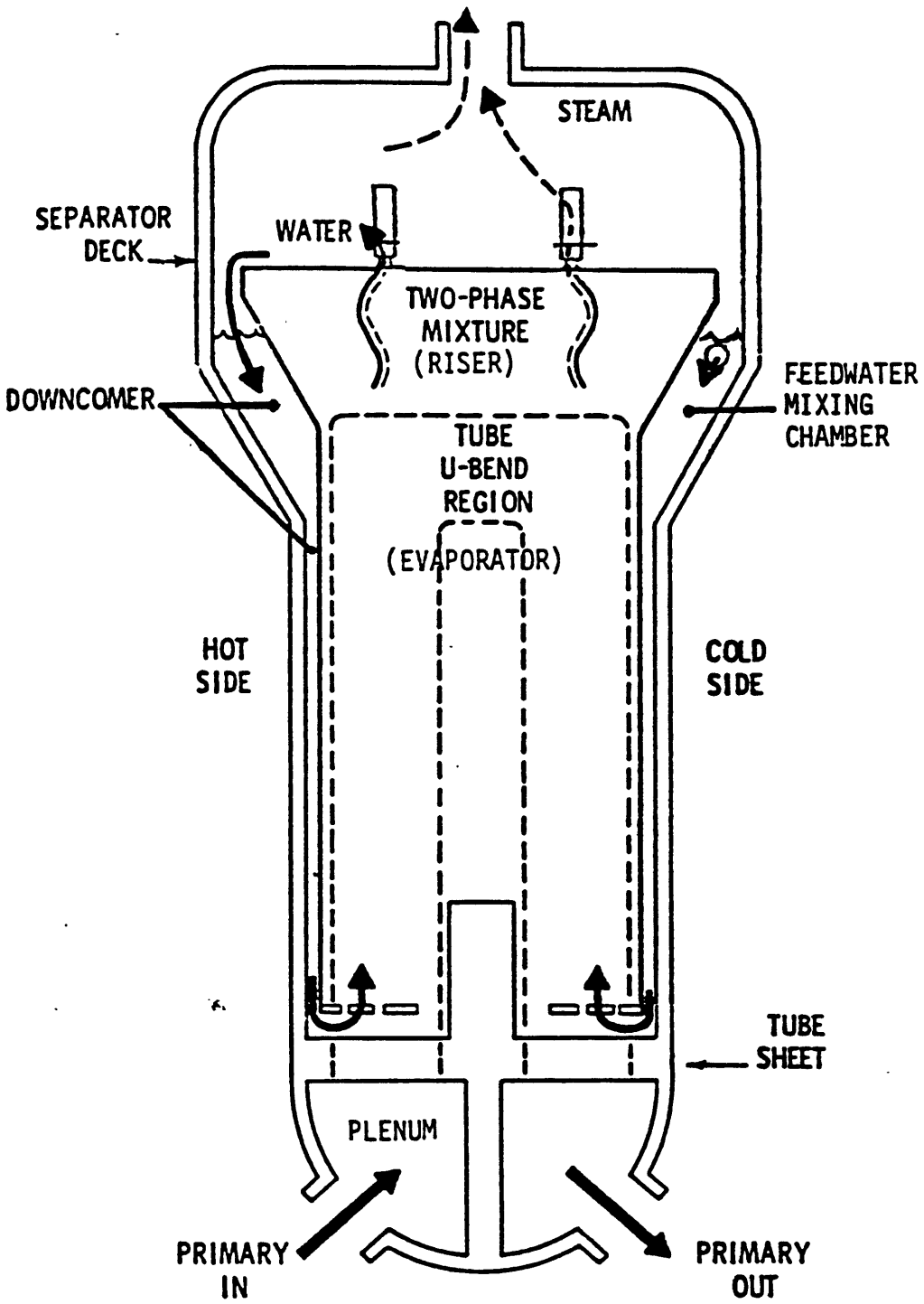

Fig. 2-1. Schematic Diagram of a U-Tube Steam Generator

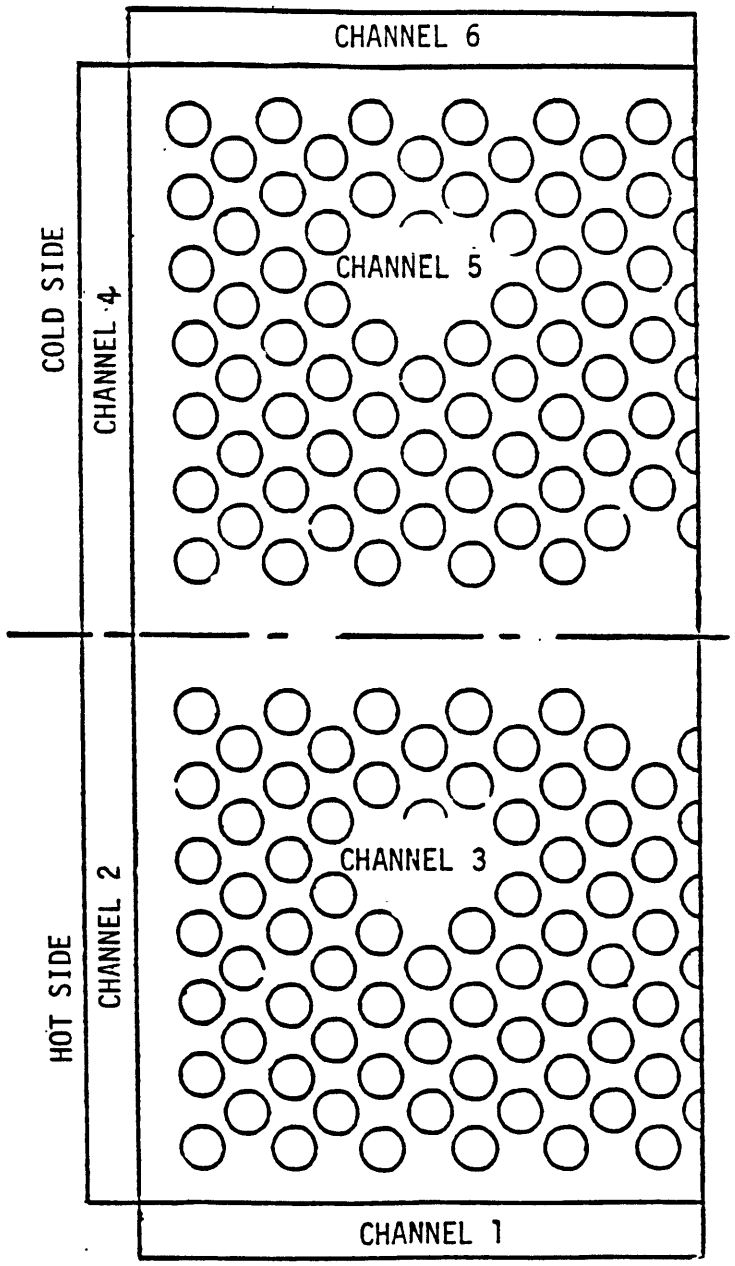

Fig. 2-2. Typical U-Tube Steam Generator Cross Section

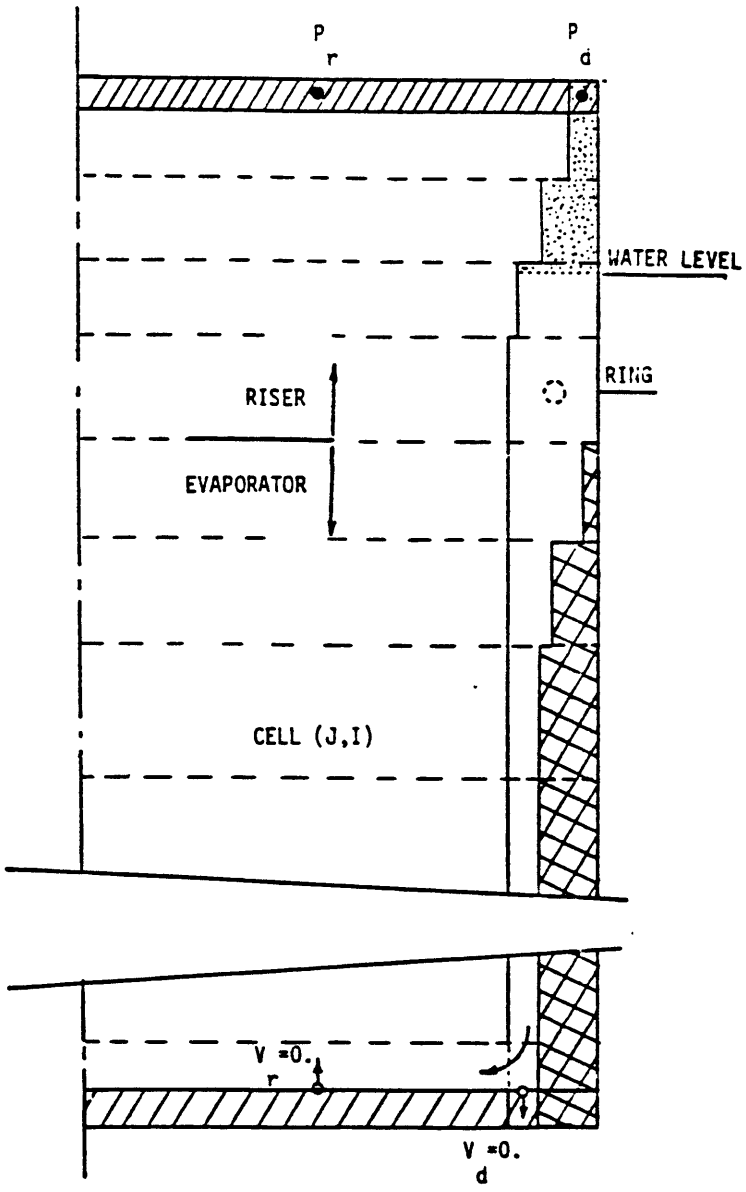

Fig. 2-3. Typical U-Tube Steam Generator Side View

III. Calvert Cliffs Steam Generator Models

The Calvert Cliffs/Unit 1 Nuclear Plant has a 2x4 loop arrangement: two hot legs and two steam generators with four cold legs and four reactor coolant pumps (RCP). The plant operates at 2700 MW_t. The steam generators are Combustion Engineering units with 8519 U-tubes of 0.02 m O.D. The distance from the tube sheet to the top of the tube bundle is 8.4 m.

The Calvert Cliffs steam generator was represented with the THERMIT-UTSG model, having four downcomer and two evaporator/riser channels in the two-fluid domain. Thirteen axial levels were specified in each of these channels. The downcomer flow is forced up into evaporator/riser at the lowest axial level. The U-tubes occupy the bottom nine levels with bends in levels 7, 8, and 9. The tubes that bend within a particular level correspond to a tube bank with a separate secondary wall temperature distribution calculated by the primary-side model. The top four levels correspond to the riser and have larger flow areas due to the absence of the U-tubes and the flaring in the actual unit. There is a flow area reduction at the top before entering the steam dome that represents the separator deck. The feedwater ring in the downcomer is at level 9.

The original version of THERMIT-UTSG was modified for the simulation of SGTR accidents. Rupture flow was modeled by including mass and energy source terms in the two-fluid equations at the location of the break. For this work the break was assumed to occur at the top of the tube bundle (level 9), and the rupture flow was considered to be symmetrically split perpendicular to the U-tubes (because of the previous assumption of geometric symmetry). Also, the rupture flow was

equally distributed between the hot and cold channels. The time-dependent mass flow rate and enthalpy for the leakage are then supplied as additional boundary conditions by the user.

The Los Alamos SGTR calculations with TRAC used a complete primary side model and a secondary-side model that included the two steam generators and their steam lines up to the turbine stop valves (TSV) and turbine bypass valves (TBV). The primary side of the U-tubes was modeled as a single flow path with 17 mesh cells. The secondary side was represented with 5 TEE components, corresponding to the: evaporator/riser, steam dome, upper downcomer, lower downcomer, and downcomer drain region. The primary flow path through these components formed a loop. The TEE side-arms represented the: rupture flow path, steam outlet, main feedwater (MFW) inlet (feedwater ring), auxiliary feedwater (AFW) inlet, and downcomer drain line, respectively. Ten cells were used to represent the evaporator/riser, four cells for the steam dome, and twelve for the downcomer. The separation of the vapor from the liquid was accomplished by using an artifically large flow area at the steam outlet. This produced a vapor velocity that was too low to entrain liquid, assuming that the flow regime in this region will always be annular or droplet. Rupture flow was initiated by opening a valve in the side-arm of the riser TEE, which connected the primary and secondary sides. Flow entered the riser in the eighth cell from the bottom which corresponded to the top of the U-tubes.

To provide a meaningful comparison of the two codes, the system boundary conditions required by THERMIT-UTSG were taken from the results of the TRAC calculation. These included the boundary conditions given in Table 2-1 and the time-dependent, rupture mass flow rate and enthalpy.

IV. Steady-State Calculation

A THERMIT-UTSG steady-state calculation was performed to provide the initial conditions for the SGTR transient calculations and to determine how well the code could match the plant operating conditions and the TRAC steady-state results. Performing a steady-state calculation with THERMIT-UTSG is a two-step process in which the steam generator boundary (operating) conditions are held constant. First, an initialization calculation is performed in which there is no recirculation flow. This supplies preliminary thermal-hydraulic conditions for the steam generator. Then, the downcomer water level is initialized and the code is run with recirculation flow. Until steady-state is reached the system will be inconsistent with the supplied boundary conditions. THERMIT imposes the supplied power and allows the primary mass flux to vary. The code iterates on the solution by running a "null transient" until a converged steady-state is found. The values of the boundary conditions used, shown in Table 4-1, were taken from the TRAC calculation.

Even when a converged steady-state is found, it may be different from that of the actual plant (or that obtained with TRAC). For example, the calculated primary mass flux may not agree with the operating value. This indicates a deficiency in the model. It is possible at this point to improve the steady-state by adjusting model parameters that may not be well known. Such parameters include: U-tube fouling factor, heat transfer areas, additive friction losses. However, there is no guarantee that adjusting any of these parameters will improve the steady-state solution. They may artifically improve agreement with some of the plant conditions while masking other model deficiencies. Such discrepancies between the model and the plant may result in very different transient responses.

TABLE 4-1

Steady-State Boundary Values

Primary Inlet Temperature	585.1 K
Primary System Pressure	15.46 MPa
Power	1358 MW
Steam Dome Pressure	5.88 MPa
Feedwater Temperature	494.8 K
Water Level	9.97 m
No Rupture Flow	

Steady-state values calculated by THERMIT are compared with the TRAC results and plant conditions in Table 4-2. The primary mass flux and primary outlet temperature calculated by both THERMIT and TRAC agree well with the plant operating conditions. This indicates that both codes are calculating the correct overall heat transfer to the secondary side. However, the secondary-side agreement is not as good. The recirculation ratio, which is the ratio of the riser flow to the outlet steam flow, is substantially different for both codes. The plant value lies between the two code values. Also, the secondary-side water inventory calculated by TRAC is close to the plant value, but the THERMIT value is much lower.

The large difference in recirculation ratios suggests that conditions within the evaporator/riser are different. The recirculation ratio is a measure of how much "dry" steam can be extracted from the two-phase mixture entering the steam dome. A low recirculation ratio indicates the outlet steam flow is large relative to the liquid flowing back into the downcomer. At steady-state all of the vapor entering the steam dome will leave the steam generator except for a small amount that will condense and be recirculated. Therefore, the recirculation ratio is primarily determined by the vapor content of the flow leaving the riser. Based on this reasoning, the riser flow should have a higher vapor content in the THERMIT calculation than in the TRAC calculation. Figure 4-1 shows the evaporator/riser void distribution for the two calculations, and indeed, this is the case. The higher recirculation flow in TRAC leads to higher fluid velocities in the evaporator/riser as shown in Figures 4-2 and 4-3 for the vapor and liquid, respectively.

TABLE 4-2

Comparison of Steady-State Results

	THERMIT-UTSG	TRAC	Calvert Cliffs Plant Conditions
Primary Mass Flux (kg/m^2-s)	5117	5062	5226
Primary Outlet Temperature (K)	559.4	559.3	559.5
Recirculation Ratio	2.14	7.09	4.0 ± 0.5
Secondary-Side Water Inventory (kg)	37,980	61,830	62,650 ± 2,250

The differences in water inventory can be explained by considering how the water was distributed in each calculation. Table 4-3 shows the geometric volume and the water inventory calculated by the two codes for the evaporator/riser, steam dome, and downcomer portions of the steam generator. There are some differences in volume and water inventory due to the different nodalizations used, but it is evident that there is much more water throughout the steam generator in the TRAC calculation, especially in the steam dome and upper downcomer, even though the total geometric volume difference is small. Therefore, the higher water inventory results from the lower voiding in the TRAC calculation.

The recirculation flow, water inventory, and amount of voiding are all interrelated. Consider a simple, steady-state, energy balance for the evaporator/riser:

$$\dot{Q} = \dot{m}\ \Delta h$$

The power $\dot{Q}$ is equal to the flow rate $\dot{m}$ times the enthalpy riser Δh. For a given power and downcomer water level, if the recirculation flow (and hence the flow throughout the system) increases, the enthalpy rise across the evaporator/riser much decrease, resulting in less voiding and a higher water inventory. The effect of decreasing the recirculation flow is just the opposite, resulting in more voiding and a lower water inventory.

The different heat transfer correlations used by THERMIT and TRAC strongly affects these interrelated quantities. Although the total amount of heat transferred to the secondary side is the same at steady-state, the evaporator flow and the enthalpy rise can vary such that the product of the two (i.e., the power) is constant. A change in heat transfer resistance at constant power would alter the secondary-side

TABLE 4-3

Comparison of Water Distributions

	Evaporator/Riser	Steam Dome	Downcomer	Total
THERMIT Model Geometric Volume (m^3)	107.7	114.9*	11.2	233.8
TRAC Model Geometric Volume (m^3)	95.3	100.7	28.2	224.2
Actual (Plant) Geometric Volume (m^3)	103.6	83.8	39.2	226.6
THERMIT Water Inventory (kg)	14,450	14,590*	8,940	37,980
TRAC Water Inventory (kg)	21,560	19,620	17,250	58,430+

*Includes upper downcomer down to the feedwater ring.

+The difference between this value and that in Table 3 is due to the water content of the five TEE side-arm pipes and the downcomer drain.

enthalpies, requiring a compensating change in flow. In the next section we will show that the different heat transfer packages do lead to different secondary-side conditions.

The different methods used by the two codes to model phase separation in the steam dome also affects these quantities. Both codes conserve mass and energy in the steam dome and both allow only pure vapor to exit. However, the TRAC model does not require that all of the vapor entering the steam dome flow out the steam line. Some of it is returned to the downcomer and is there condensed by the cold feedwater. An examination of the TRAC results showed that the void fraction of the recirculation flow is only slightly lower than the flow entering the steam dome. This indicates that not enough phase separation is occurring, resulting in a larger recirculation flow and less voiding in the evaporator/riser. Since the recirculation flow is too high, the good agreement between the TRAC water inventory and that in the plant is probably fortuitous. Reference 1 states the heat transfer areas were adjusted to improve agreement with plant operating conditions. However, this could have masked the problem with the steam dome model, improving the steady-state agreement (e.g., the water inventory) but adversely affecting how the system will behave under transient conditions. These things should be given further consideration.

THERMIT predicts that the boiling front is lower in the hot channel than in the cold channel (see Figure 4-1). However, midway up the evaporator this asymmetry is reversed with the cold-channel void exceeding that in the hot channel. Here also, the cold-channel vapor and liquid velocities exceed those in the hot channel as shown in Figures 4-2 and 4-3. These results are due to the strong crossflow from

the hot channel to the cold channel, shown in Figure 4-4. The crossflow is driven by small pressure differences arising from temperature differences, between the two channels. The crossflow is positive (hot to cold channel) along the heated length but reverses above the U-tubes in the riser. The crossflow tends to homogenize the two channels, indicating that a one-dimensional model of the evaporator/riser may be adequate at steady-state if the heat transfer and friction factor correlations used were based on U-tube bundle data.

In the riser there is an increase in flow area due to the absence of the U-tubes as well as a flaring of this section. This expansion causes both the vapor and liquid velocities in the riser to decrease to the point that the interfacial drag is no longer sufficient to overcome the gravitational force on the liquid and the liquid falls back down. This produces a slight decrease in void fraction in this region. The area constriction representing the separator deck at the riser exit sharply increases the fluid velocity as it enters the steam dome region.

Because the primary mass flux was close to the plant value and that obtained by TRAC, no U-tube fouling was considered, i.e., the fouling factor was set equal to one. If the mass flux had been too low, the addition of tube fouling would have increased the heat transfer resistance of the wall metal, requiring a higher primary mass flux to transfer the same power. However, tube fouling would not have had a significant effect on the secondary-side conditions, since the heat transfer resistance of the wall to secondary-side fluid is low (boiling) compared with that of the primary fluid to wall or conduction through the wall. The results of the next section where tube fouling was considered support these observations. Adjusting the heat transfer area

would have provided an even coarser means of improving the steady-state calculation, since the heat transfer area is directly proportional to the power. Similarly, the additive friction losses on the secondary side would have affected the flow rate, which determines the heat removal capability of the evaporator. Adjustment of either of these parameters would have affected both primary and secondary-side conditions.

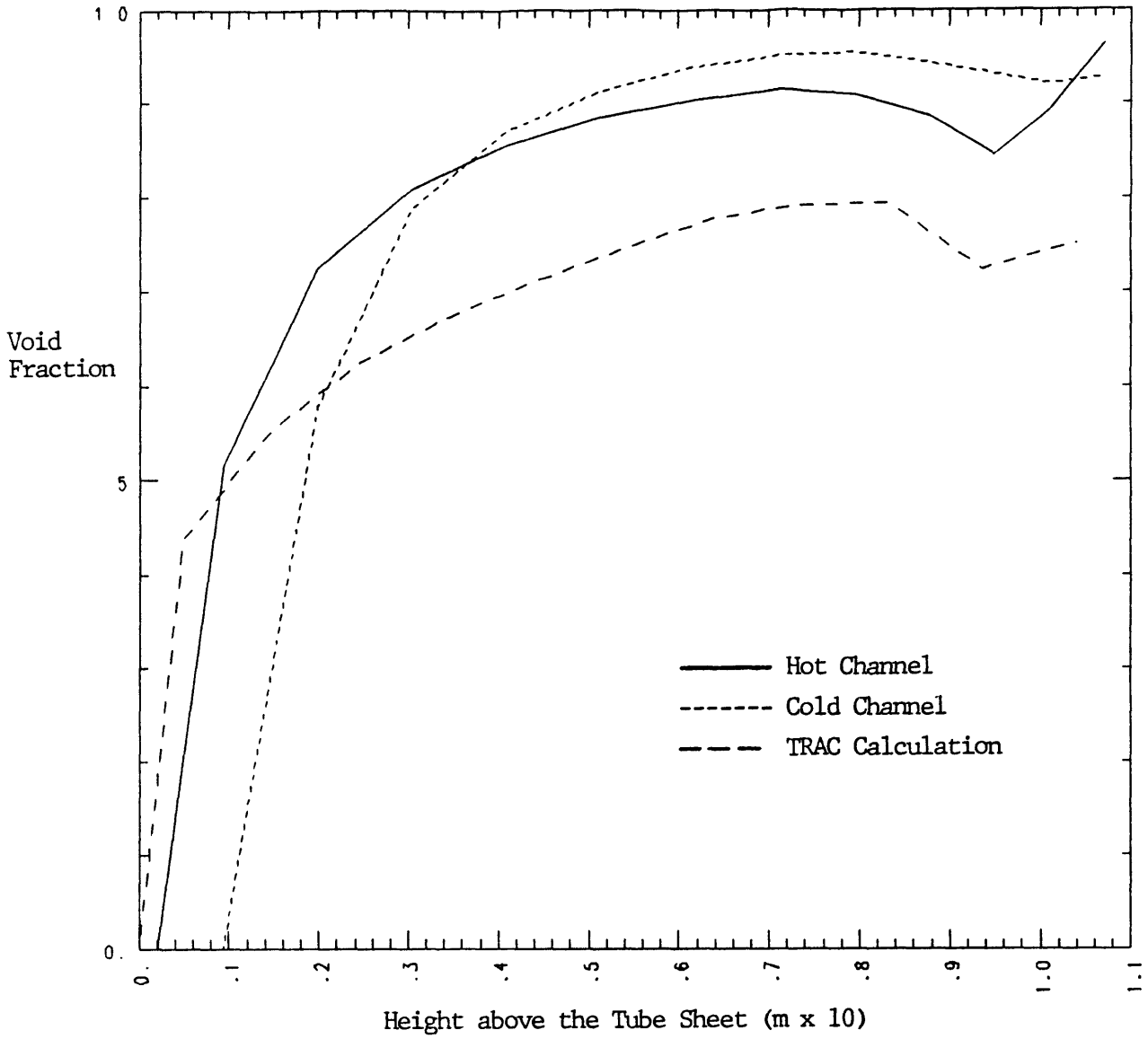

Fig. 4-1. Evaporator/Riser Void Fraction Distribution

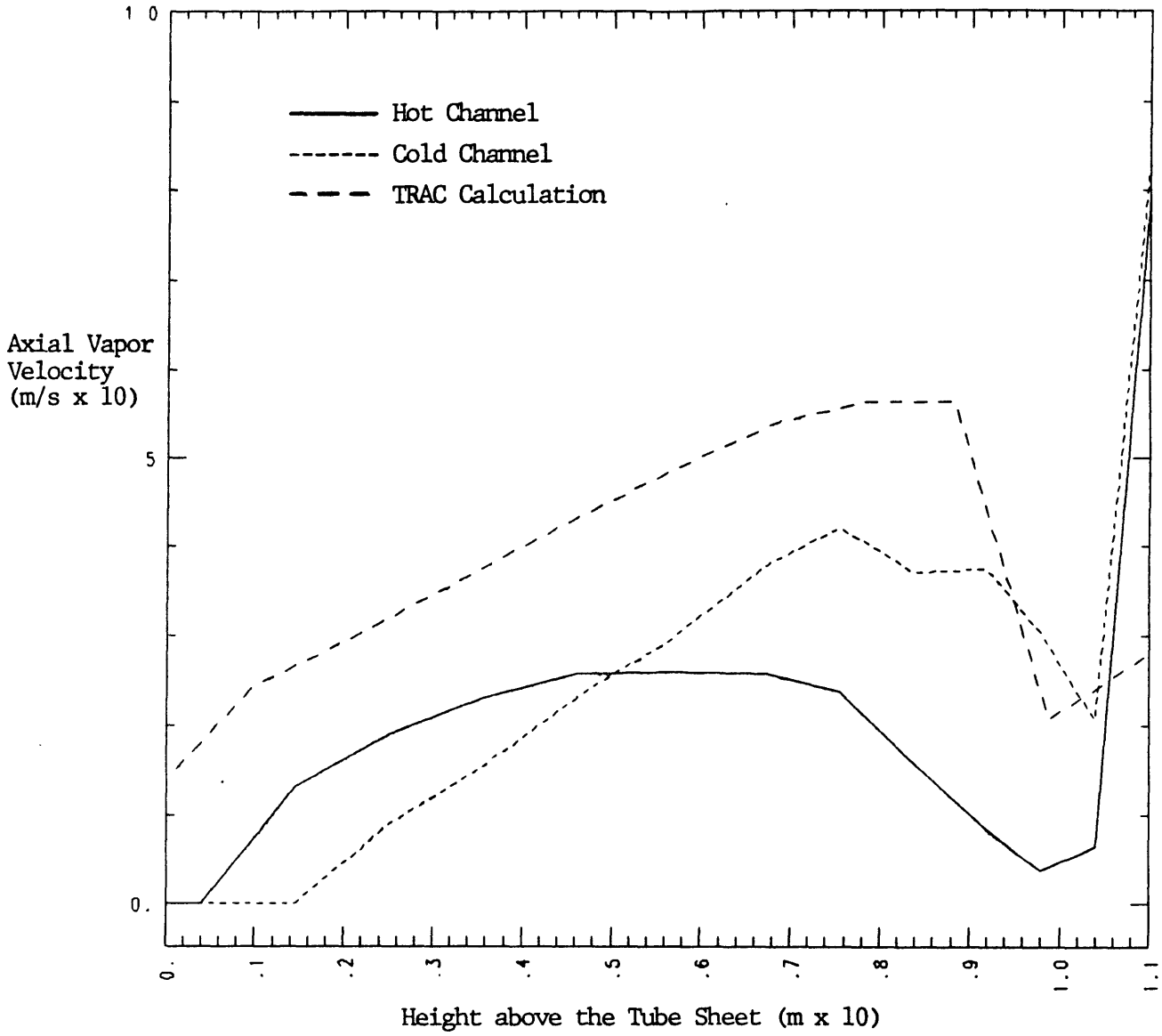

Fig. 4-2. Axial Vapor Velocity Distribution

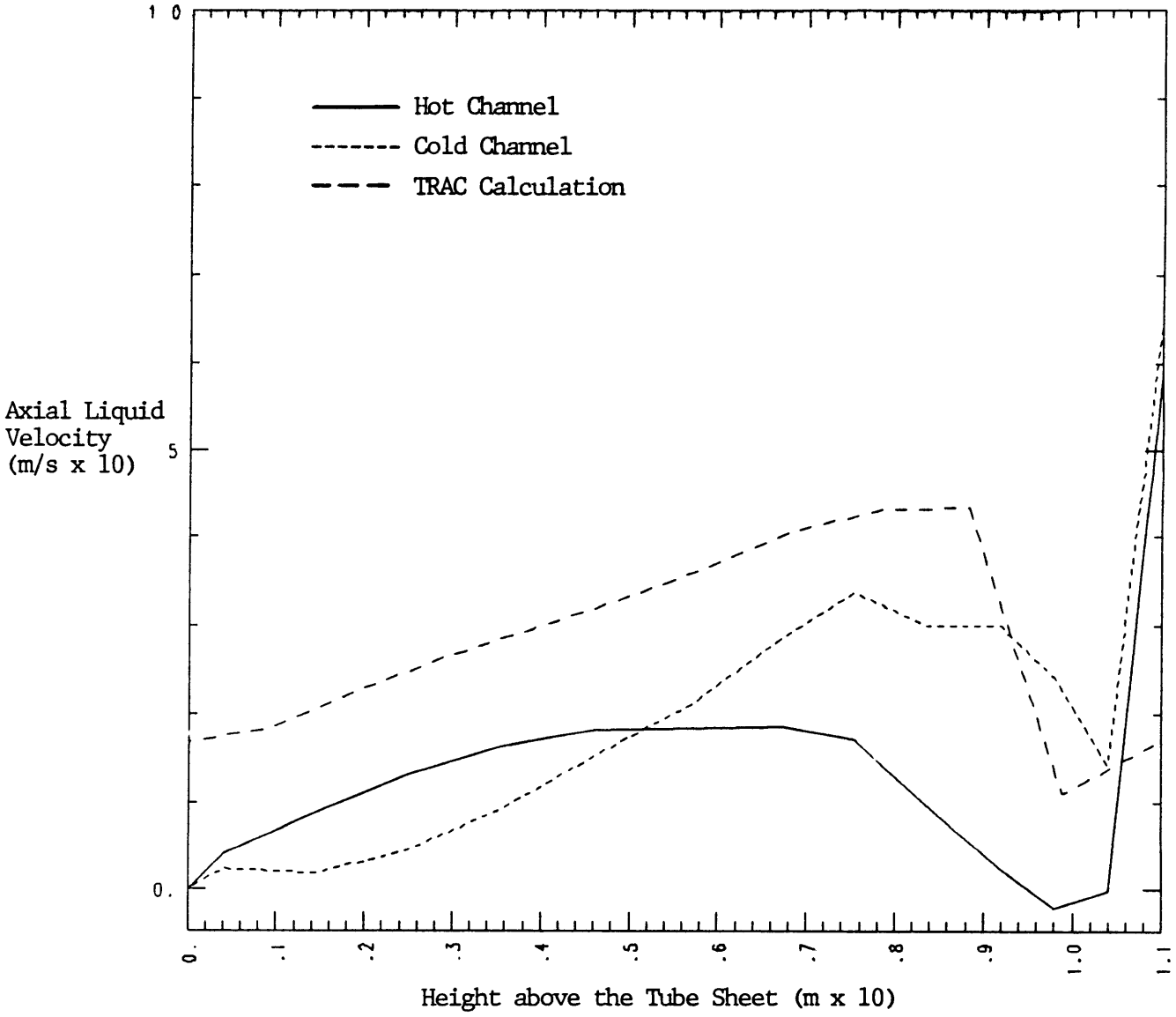

Fig. 4-3. Axial Liquid Velocity Distribution

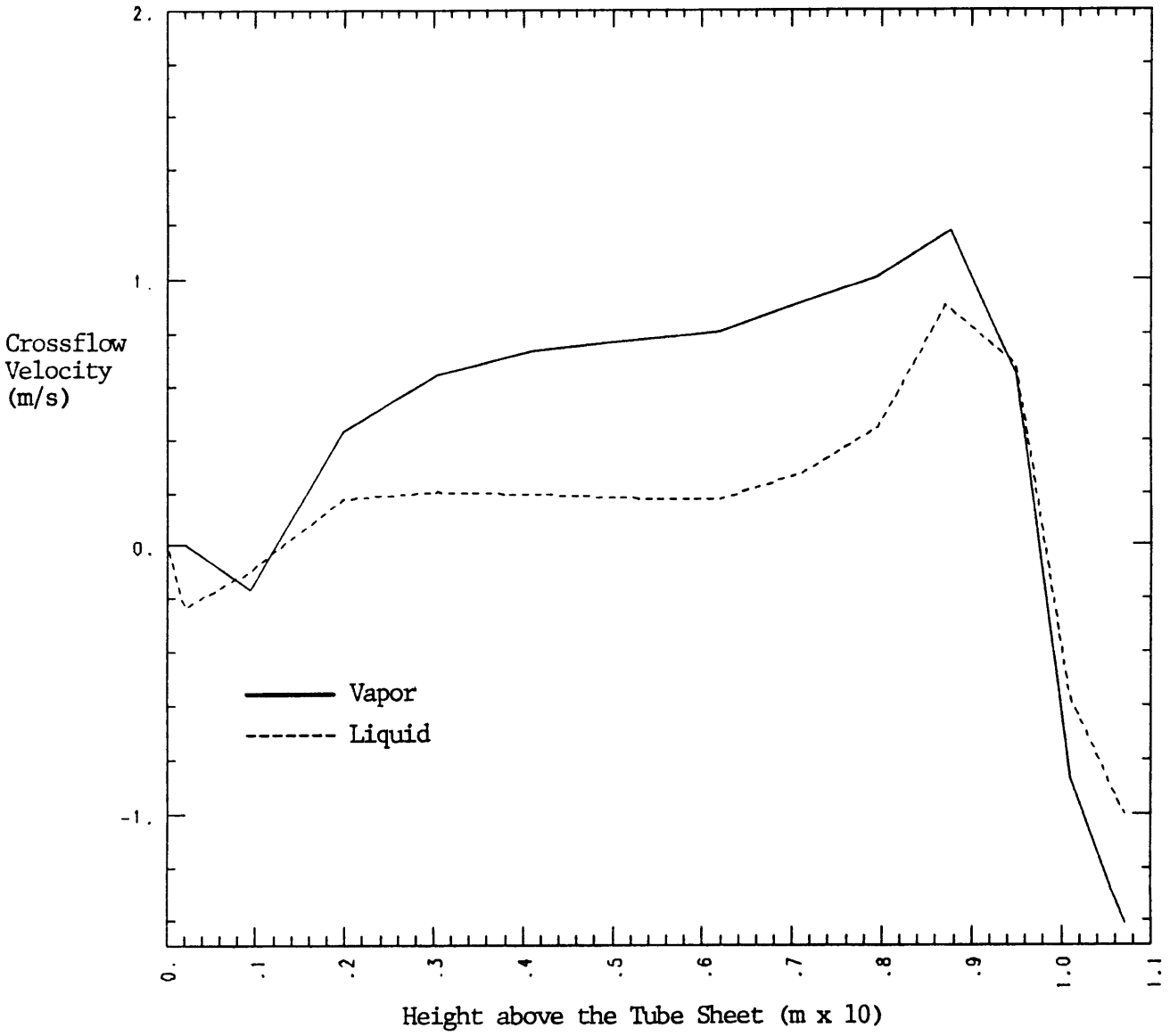

Fig. 4-4. Evaporator/Riser Crossflow Velocity Distribution

V. Heat Transfer Study

A major difference between the THERMIT and TRAC codes is the set of heat transfer correlations used. To assess the impact of this difference on the results of the two codes, we replaced the THERMIT heat transfer correlations with those used by TRAC. This special version of THERMIT-UTSG was used to repeat the steady-state calculation.

In this section we compare the correlations used by the two codes for various heat transfer regimes and then present the results of the steady-state calculation run with this modified version of THERMIT-UTSG.

V.1 TRAC-PF1 and THERMIT-UTSG Heat Transfer Correlation Comparison

The following comparison attempts to point out the essential features of the two heat transfer packages. For additional details, the reader should consult the appropriate code manuals.

Single-Phase Liquid

In forced convection mode, TRAC uses the maximum of the laminar and turbulent correlations,

$$\text{laminar:}\quad h_\ell = 4.0\, k_\ell/D_h \quad (\text{i.e., } Nu_\ell = 4.0)$$

$$\text{turbulent:}\quad h_\ell = 0.023\, k_\ell/D_h\, Re_\ell^{0.8}\, Pr_\ell^{0.4} \quad \text{(Dittus-Boelter)}$$

In TRAC, forced convection is assumed when the ratio of the Grasshoff number to the Reynolds number squared is less than one; otherwise natural convection is assumed to be the appropriate regime.

For natural convection, TRAC employs the maximum of the laminar and turbulent Nusselt numbers for vertical flat plates and cylinders, with,

$$Nu_\ell = 0.59\, (Gr_\ell\, Pr_\ell)^{0.25}$$

for laminar flow and

$$Nu_\ell = 0.10\ (Gr_\ell\ Pr_\ell)^{0.333}$$

for turbulent flow.

THERMIT does not account for laminar flow and simply uses the maximum of the Sieder-Tate correlation

$$Nu_\ell = 0.023\ Re_\ell^{0.8}\ Pr_\ell^{0.33}\ (\mu_\ell/\mu_w)^{0.14}$$

and McAdams correlation:

$$Nu_\ell = 0.13\ \ (Gr_\ell\ Pr_\ell)^{0.333}$$

Single-Phase Vapor

TRAC uses the maximum of Dittus-Boelter and McAdams correlations while THERMIT uses the maximum of Sieder-Tate and McAdams correlations.

Nucleate Boiling

For its liquid heat transfer coefficient, TRAC uses the Chen correlation, which is composed of a forced convection (macroscopic) term and a nucleate boiling (microscopic) term. The forced convection term is identical to the forced convection term used in the single-phase liquid regime, except that it is multiplied by the Reynolds F factor.

Both THERMIT and TRAC use the same nucleate boiling term, which also contains a nucleation suppression factor.

The liquid heat transfer coefficient for TRAC is

$$h_\ell = h_{fc} + \text{Min}\left(1, \frac{t_w - t_{sat}}{t_w - t_\ell}\right) h_{nucb}$$

TRAC also uses a non-zero vapor coefficient given by

$$h_g = \left(\frac{t_w - t_s}{t_{chf} - t_s}\right)^2 \text{Max}\ (h_{fbb}, h_{nc}, h_{dr})$$

where h_{fbb}, h_{nc}, and h_{dr} are the Bromley, natural convection, and Doughall-Rohsenow coefficients, respectively.

The total heat flux in THERMIT is given by

$$q_{total} = h_{fc}(t_w - t_\ell) + h_{nucb}(t_w - t_s)$$

i.e., there is no vapor heat transfer in this regime.

Transition Boiling

In this regime the TRAC package performs a quadratic interpolation between the critical heat flux and the minimum stable film boiling heat flux. It calculates the vapor heat transfer coefficient as

$$h_g = \text{Max}(h_{fbb}, h_{nc}, h_{dr})$$

and then determines the liquid heat transfer coefficient from the total heat flux and h_g

$$h_\ell = \frac{q_{total} - h_g(t_w - t_v)}{(t_w - t_\ell)}$$

THERMIT performs a linear interpolation between the heat fluxes at the minimum stable film boiling point and critical heat flux point.

Film Boiling

TRAC employs a radiative and a dispersed flow component for its liquid heat transfer coefficient:

$$h_\ell = \left(\frac{t_w - t_s}{t_w - t_\ell}\right) h_r + h_{df}$$

TRAC's vapor heat transfer coefficient is the maximum of the Bromley, natural convection, and Doughall-Rohsenow values.

The Bromley coefficient is identical to the modified Bromley coefficient used in THERMIT's film boiling regime.

In the THERMIT version adapted to steam generator analysis, film boiling heat transfer is greatly simplified compared to the "original" THERMIT. Specifically, if the wall temperature exceeds the minimum stable film boiling temperature, convection to single-phase vapor is assumed.

Critical Heat Flux Calculation

TRAC uses the Biasi forced flow correlation to obtain the critical heat flux, q_{CHF}. Once q_{CHF} is determined, the temperature corresponding to the CHF point is calculated using a Newton-Raphson iteration to determine the intersection of the heat flux found by using the nucleate boiling heat transfer coefficient (Chen correlation) and the critical heat flux.

THERMIT uses the Biasi forced flow correlation for a mass flux, G, greater than 270 kg/m^2-sec. If G is less than or equal to 27 kg/m^2-sec the CHF-Void correlation is used:

$$q_{CHF} = 0.1178(1 - \alpha)h_{g\ell}[\sigma_g(\rho_\ell - \rho_v)\rho_v^2]^{0.25}$$

For $27 \leq G \leq 270$, linear interpolation is used between the Biasi correlation at 270 and the CHF-Void correlation of 27.

A Newton-Raphson method is again used to obtain the critical heat flux temperature from the nucleate boiling coefficient.

Minimum Stable Film Boiling Heat Flux Calculation

TRAC applies the homogeneous nucleation minimum stable film boiling temperature correlation:

$$t_{Min} = t_{nh} = (t_{nh} - t_{\ell})R^{0.5}$$

$$R = (k\rho c)_{\ell}/(k\rho c)_{w}$$

t_{nh} = homogeneous nucleation temperature, which is given by Fauske and a curve fit to these results.

Once t_{Min} is known, the corresponding heat flux q_{Min} is calculated as:

$$q_{Min} = h_{\ell_{Min}} (t_{Min} - t_{\ell}) + h_{g_{Min}} (t_{Min} - t_{v})$$

where $h_{\ell_{Min}}$ and $h_{g_{Min}}$ are the liquid and vapor heat transfer coefficients evaluated using the film boiling correlations at temperature t_{Min}.

THERMIT uses a slightly different correlation for t_{Min}

$$t_{Min} = t_{nh} + (t_{nh} - t_{\ell})R^{0.5} + \psi(P)$$

where

$$\psi(P) = \begin{cases} 0 & p \geq 4.826 \times 10^{5} \text{ Pa} \\ 127.3 - 26.37 \times 10^{-5} p & p < 4.826 \times 10^{5} \text{ Pa} \end{cases}$$

and

$$t_{nh} = \begin{cases} 581.5 + 0.01876(p - 1.034 \times 10^{5})^{-5} & p \leq p_{o} \\ 630.39 + 0.004321(p - p_{o})^{0.5} & p > p_{o} \end{cases}$$

$$p_{o} = 68.95 \times 10^{5} \text{ Pa}$$

Once t_{Min} is calculated, the heat flux is determined exactly as it is in the TRAC package.

Convection to Two-Phase Mixture Regime

TRAC allows for the separate calculation of the heat transfer coefficients when critical heat flux cannot occur.

The liquid coefficient is given by the maximum of the laminar and turbulent coefficients for single-phase liquid, evaluated with a two-phase viscosity from McAdam's equation:

$$\mu_M = \frac{1}{\frac{x_f}{\mu_g} + \frac{(1 - x_f)}{\mu_\ell}} \qquad \text{where } x_f = \text{flow quality}$$

If the void fraction is less than or equal to 0.98, the vapor coefficient is zero. If the void fraction is greater than 0.98, then $h_\ell = 0$ and h_g is the greater of the natural convection and turbulent coefficients in the film boiling regime.

There is a similar (but not exact) counterpart of this type of calculation in THERMIT, where a bypass of the transition boiling under steady-state conditions is performed, thereby precluding CHF.

Condensation Regime

TRAC applies the Chen correlation with a zero value for the suppression factor. If the equilibrium quality is greater than 0.71 then the Chen correlation is evaluated at $x = 0.71$ with $h_g = 0$. Linear interpolation is used between these values and the single-phase vapor values ($h_\ell = 0$).

THERMIT applies the single-phase liquid heat transfer coefficient.

V.2 Steady-State Results

A special version of THERMIT-UTSG containing the TRAC heat transfer correlations was created. This version of the code was used to repeat the steady-state calculation. Comparing these results with those given previously in Section IV, helps to isolate the effect of the different heat transfer packages and allows a closer comparison of the two codes.

The first column of Table 5-1 lists the calculated values of important steady-state quantities. These should be compared with the values of the previous THERMIT and TRAC calculations and the plant operating conditions shown in Table 4-2. The values of the primary mass flux and outlet temperature are both significantly lower than those in the previous calculations, which matched the primary-side operating conditions well. This indicates that either the heat transfer resistance is too low or the heat transfer area is too high. These results were obtained assuming no tube fouling (fouling factor = 1.0). To obtain better agreement of the primary-side results, the calculation was repeated using a fouling factor > 1. A fouling of 1.22 was found to give good agreement with the TRAC results for the primary-side conditions (see the second column of Table 5-1.)

The recirculation ratio is not significantly affected by the variation in fouling factors. However, it is definitely affected by the heat transfer correlations. Changing the heat transfer correlations produces the same effect as changing the heat transfer area. THERMIT with the TRAC heat transfer package gave a recirculation ratio between the previous THERMIT and TRAC calculations and close to the plant value. The water inventory was also improved substantially although it is still lower than the TRAC or plant values.

The higher recirculation ratio (indicating a higher secondary-side flow) and water inventory suggest that there is less void in the evaporator/riser. Figure 5-1 shows that this is indeed the case. The void distribution is much closer to that calculated by TRAC. The larger recirculation produces larger flow through the evaporator/riser as the vapor and liquid velocity profiles, shown in Figures 5-2 and 5-3,

TABLE 5-1

Steady-State Results of THERMIT-UTSG
with the TRAC Heat Transfer Package

	Fouling Factor = 1.0	Fouling Factor = 1.22
Primary Mass Flux (kg/m^2-s)	4590	5044
Primary Outlet Temperature (K)	556.3	559.1
Recirculation Ratio	4.41	4.45
Secondary-Side Water Inventory (kg)	47,400	47,200

respectively, indicate. The stronger axial flows tend to increase the hot/cold channel asymmetry. Notice that the void fraction and velocity differences between the two channels are much greater than previously calculated by THERMIT, using the THERMIT heat transfer correlations. The void fraction and the velocity in the cold channel never exceeds that in the hot channel within the evaporator section. The crossflows, shown in Figure 5-4, are also much lower (especially relative to the axial flow) and reverse (flow from cold to hot side) below the top of the U-tube bundle.

The different heat transfer correlations used by THERMIT and TRAC produce significant differences in the steady-state results. When the TRAC heat transfer package was used in THERMIT, the steady-state results were in better agreement with the TRAC results and the plant operating conditions. Only the water inventory is still low. The good agreement of the recirculation ratio with the plant value provides further evidence of the phase separation problem with the TRAC model discussed in Section IV. Also, the multidimensional effects are more pronounced because of the stronger axial flows, relative to the crossflow. Since the flow rates were close to those expected in the actual plant, a one-dimensional model may not adequately represent the system.

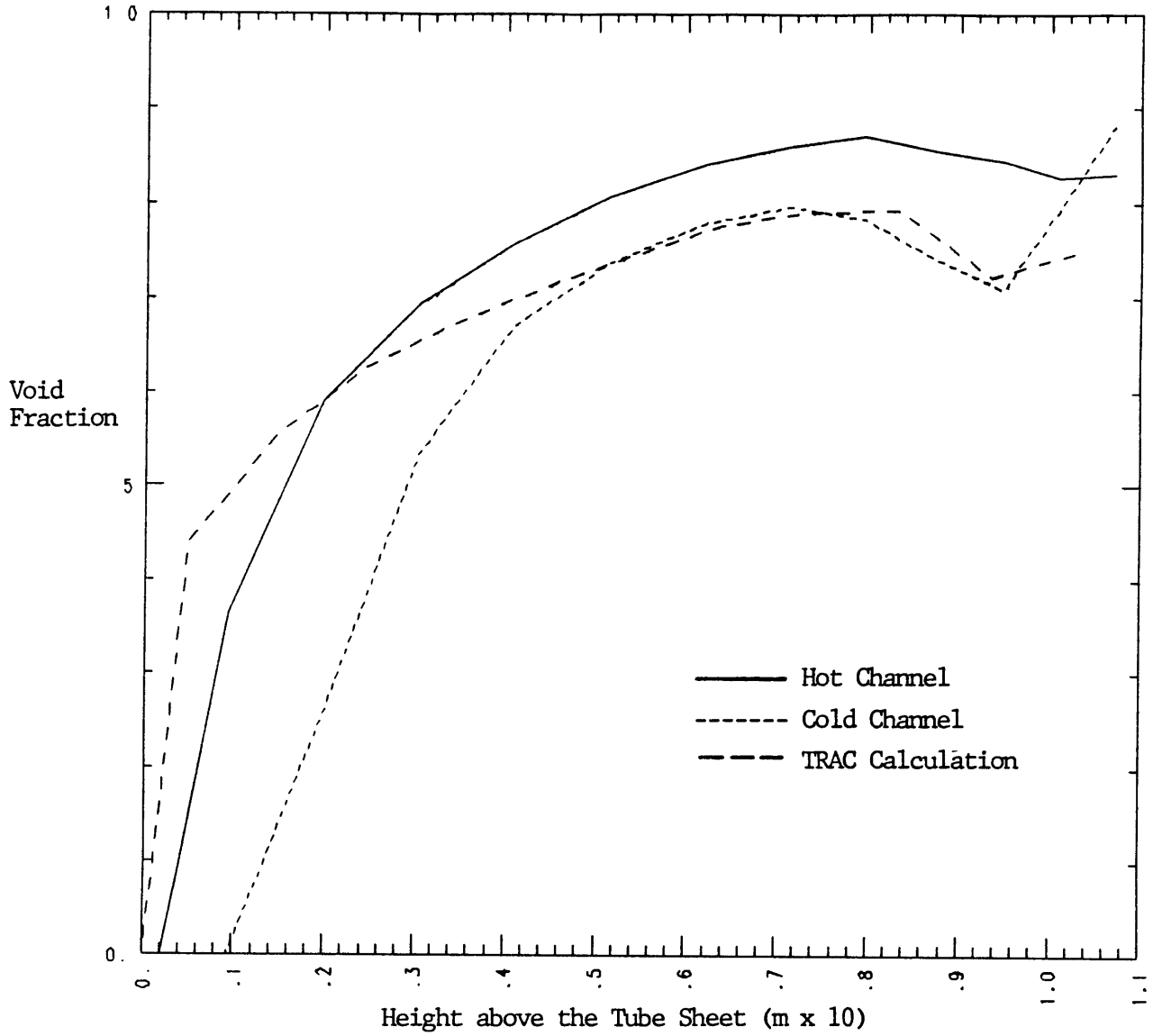

Fig. 5-1. Evaporator/Riser Void Fraction Distribution: TRAC Heat Transfer (Fouling Factor = 1.22)

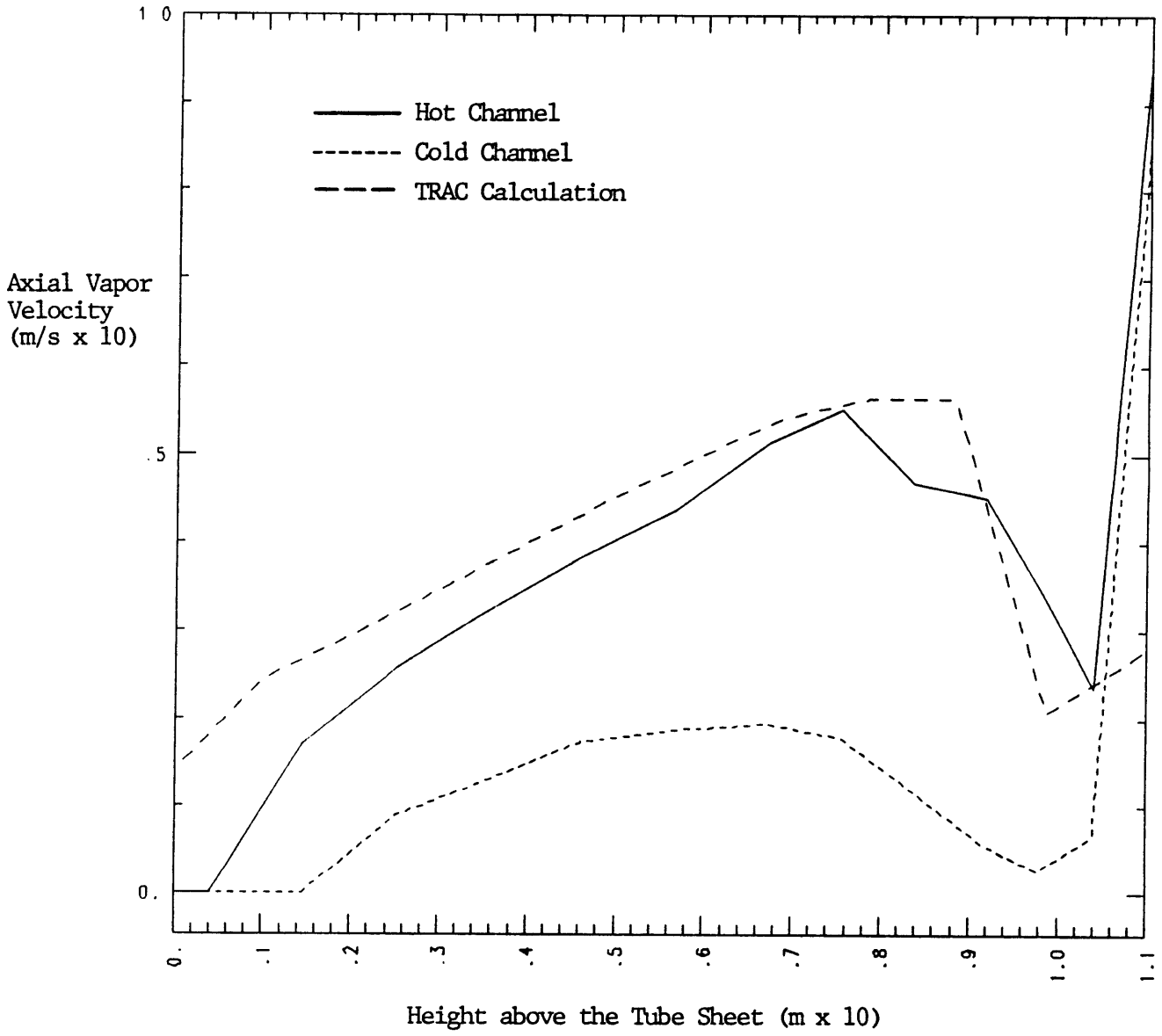

Fig. 5-2. Axial Vapor Velocity Distribution: TRAC Heat Transfer (Fouling Factor = 1.22)

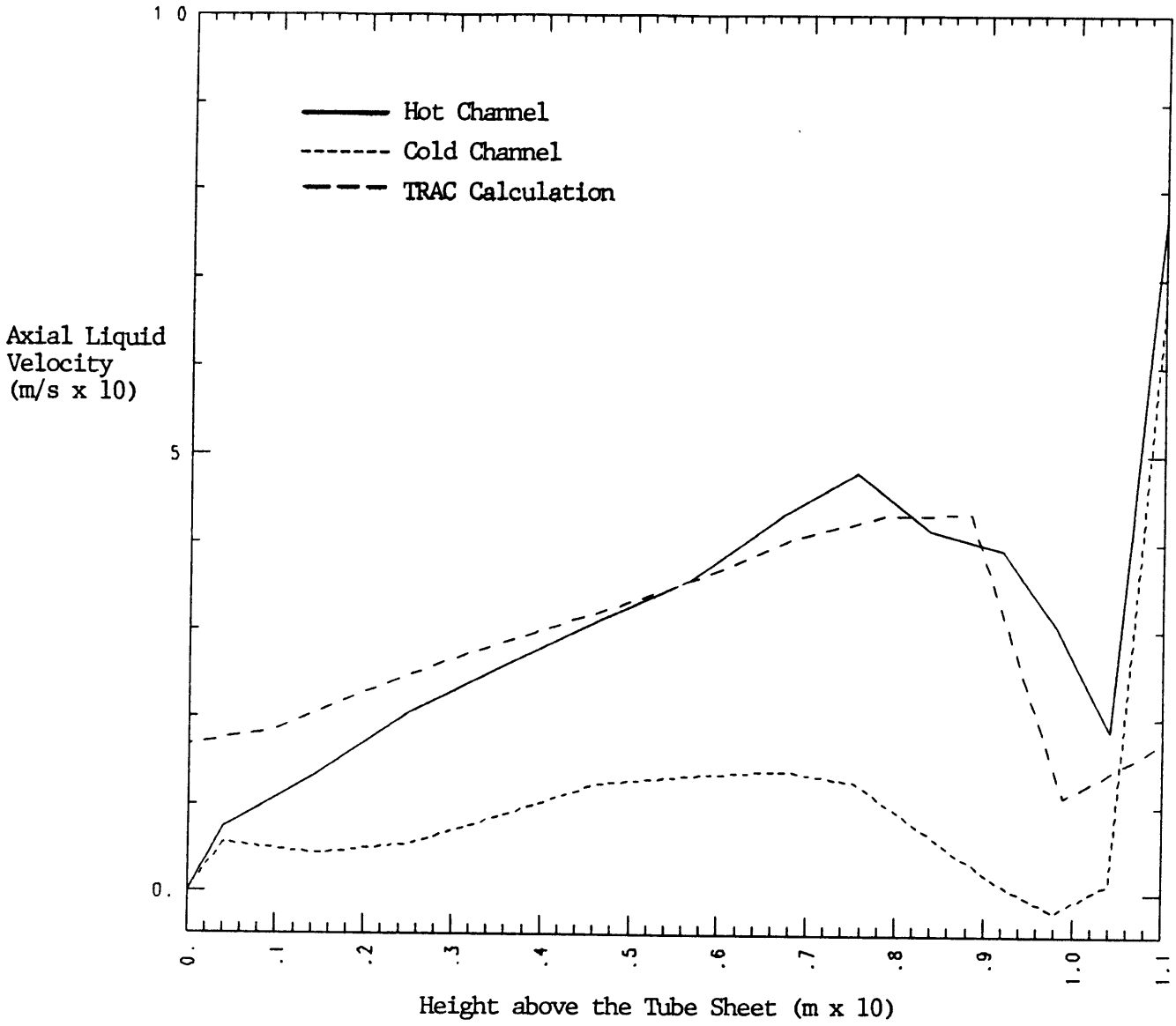

Fig. 5-3. Axial Liquid Velocity Distribution: TRAC Heat Transfer (Fouling Factor = 1.22)

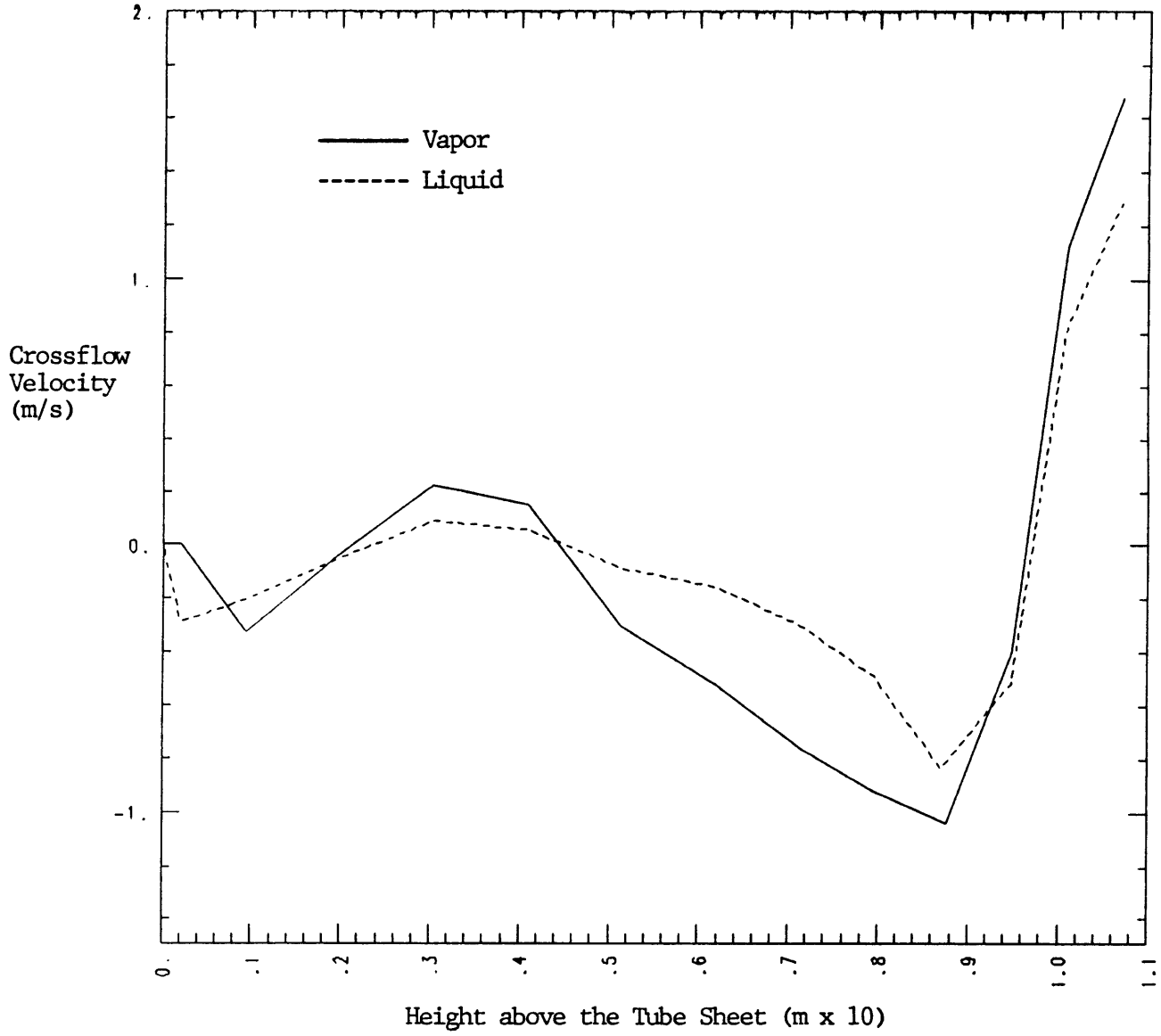

Fig. 5-4. Evaporator/Riser Crossflow Velocity Distribution: TRAC Heat Transfer (Fouling Factor = 1.22)

VI. Transient Calculations

The SGTR study performed at LANL investigated the system response of the Calvert Cliffs Nuclear Plant to five postulated accident scenarios [1]. We have run two of these five scenarios using THERMIT-UTSG to provide an independent assessment of their calculations. In this section we describe the two scenarios that we studied, designated Case 1 and Case 3 in Reference 1, and report our results. The Case 1 scenario that we ran was a variation of the one reported in Reference 1.

VI.1 Case 3

This scenario assumed a SGTR incident in the Calvert Cliffs Nuclear Plant, operating normally at 100% power. The rupture was assumed to be a double-ended break of a single U-tube at the top of the bundle, occurring at time zero. Following the rupture, the primary system depressurized slowly, due to the leakage to the secondary side, until the reactor scrammed on low system pressure. Upon reactor scram the turbine bypass and stop valves (TBV and TSV) were closed and the main feedwater was shut off over a 60 second interval. After the turbine trip, the secondary-side pressure increased sharply, causing the atmospheric dump valves (ADV) and the safety relief valves (SRV) to open. The primary system continued to depressurize, leading to reactor coolant pump (RCP) trip on low pressure. In this particular scenario only two of the four RCPs were shut off (one in each loop). Following RCP trip, normal operator action was taken to isolate the damaged steam generator. The sequence of system and operator events for this scenario is shown in Table 6-1. The LANL work showed that if the high pressure

TABLE 6-1

System and Operator Events for Case 3

Time (s)	Event
<0	Full power, steady-state operation
0	SGTR
574	Pressurizer heaters off on low pressurizer level
928.29	Reactor trip (scram) on low primary pressure (13.0 MPa)
	TSVs and TBVs close; condenser unavailable
	MFW trip: flow coastdown over next 60 s
	ADVs and SRVs open on high secondary-side pressure
988	MFW off
1000	Operator manually sets ADVs open
1028	SRVs close
1076	2 of the 4 RCPs trip on low primary pressure (9.065 MPa)
1140	Operator closes MSIV
1200	Operator closes ADVs
1220	SRVs open on high steam line pressure (6.9 MPa)
1260	Operator closes MFWIV
1320	Operator closes AFWIV
1380	Operator verifies damaged steam generator isolation
1440	Operator turns pressurizer spray on to reduce primary system pressure
1590	SRVs are essentially closed (very low steam flow)

injection is not turned off late in the transient, this scenario results in prolonged leakage and steam generator overfill.

The transient boundary conditions listed in Table 2-1 and the rupture flow rate and enthalpy were taken from the TRAC results for this scenario. This allows a back-to-back comparison of the THERMIT and TRAC code results. However, since the component response of the THERMIT steam generator model will be different from the TRAC model, the feedback of this different response through the rest of the system will not be reflected in the specified boundary conditions. This is unfortunate since to some extent it forces the THERMIT model to behave like the TRAC model. However, this problem is a limitation of any component analysis.

The transient boundary conditions up to 2400 s are shown in Figures 6-1 to 6-7. The feedwater temperature is constant throughout the transient at 494.8 K. The rupture flow temperature is shown instead of the enthalpy. The enthalpy supplied to the code was calculated from the temperature and pressure using the THERMIT water property routine. Except for the primary-side pressure and rupture flow rate, the boundary conditions are nearly constant up to scram at 928.29 s. There is a sharp change in all quantities immediately after scram except for the primary mass flux, which drops sharply after RCP trip at 1076 s. Following RCP trip, there is a brief rise in primary pressure and rupture flow. After 1600 s the flow out the SRVs is negligible and the steam dome pressure boundary condition was replaced with a zero steam flow condition. This was necessary to prevent THERMIT from calculating a negative steam flow after this time.

Using these boundary conditions the Case 3 SGTR transient was run for 2400 s (40 min) of real time with THERMIT-UTSG (the version with the THERMIT heat transfer package). A synopsis of both the THERMIT and TRAC results is given in the Appendix. The system and operator events, listed in Table 6-1, are also shown there for reference. Graphs of selected results are shown in Figures 6-8 to 6-21.

From the time of tube rupture until reactor scram at 928.29 s, conditions either change very slowly or not at all. The heat transfer rate to the secondary side (Figure 6-8) and the outlet steam flow (Figure 6-9) are nearly constant during most of this period. However, there is a small difference between the THERMIT and TRAC values, which were identical at steady-state. This is partially due to the different primary mass fluxes computed at steady-state. In transient calculations THERMIT no longer imposes the power but calculates it based on the supplied conditions. The mass flux, which is allowed to vary at steady-state, is imposed as a boundary condition at time zero. Since the mass flux taken from the TRAC calculation is slightly lower than that calculated by THERMIT, there is a small reduction in power shortly after tube rupture. The reduction in power should reduce the steam flow. However, this decrease is offset by additional vaporization resulting from the rupture flow. The THERMIT steam flow, therefore, remains nearly unchanged after tube rupture, while the TRAC steam flow shows a small increase.

The behavior of the downcomer and riser flows (Figures 6-10 and 6-11) is different in the two code calculations. THERMIT predicted a slowly decreasing flow prior to scram, while TRAC predicted increasing flow. One might think that the flow on the secondary side should be

increasing because of the leakage. The liquid rupture flow is less enthalpic than the highly voided two-phase mixture at the top of the tube bundle. It reduces the riser void fraction and decreases the steam flow with more liquid being recirculated. However, the unvaporized rupture flow, which is recirculated, has the same effect as a hot feed source, thereby lowering the boiling front in the evaporator and increasing the evaporator/riser void. Because the rupture flow is very small (<20 kg/s) compared to either the feed flow (740 kg/s or the secondary-side flow (1600 kg/s), its impact is very small as the slope of the THERMIT curves in Figures 6-10 and 6-11 indicates. The resulting increase in steam flow apparently offsets the decrease in flow due to the steady-state primary mass flux mismatch mentioned above, leaving the steam flow nearly unchanged. If there were no mismatch in steady-state mass flux, the THERMIT steam flow should increase slightly as in TRAC.

The problem with the TRAC phase separation method, discussed in Section IV, is probably responsible for the increase in flow in their calculation. Not all of the vapor is removed in the steam dome. A significant fraction of it is returned to the downcomer where it is condensed by the feedwater. This results in a slow warming of the downcomer fluid and an accumulation of mass in the system. Figure 6-12 shows that almost 10,000 kg of water accumulates on the secondary side in the TRAC calculation before scram. THERMIT predicted a slight decrease in water inventory and downcomer water level (Figure 6-13) during the same period. We expect the decrease would have been larger if there were no primary mass flux mismatch at steady-state.

The void fraction distribution in the evaporator/riser remains nearly constant before scram (compare Figures 4-1 and 6-16). The basic

shapes of these profiles are the same as calculated at steady-state. There is a slight decrease in void in the TRAC calculation, resulting from the water accumulation.

After reactor scram the heat transfer rate to the secondary-side of the steam generator drops to a low level in response to the sudden decrease in reactor power. Figure 6-8 shows that the heat transfer rate computed by THERMIT is slightly greater than that computed by TRAC until very late in the transient (~2250 s). The downcomer and riser flows (Figures 6-10 and 6-11) also drop sharply due to the decreasing MFW flow and the pressure rise following turbine trip. However, by 1000 s the flows computed by THERMIT are nearly zero compared to about 1600 kg/s given by TRAC. The TRAC flows at that time are still as high as the flows predicted by THERMIT at steady-state. The outlet steam flow rate (Figure 6-9) also falls in response to the power drop. The THERMIT steam flow follows closely the trend predicted by TRAC but is lower than the TRAC value after 1000 s. The steam flow computed by THERMIT is controlled primarily by the steam dome pressure, which is supplied as a boundary condition. No account is taken for the hydraulic resistance at the steam line entrance. This might have produced the slight difference between the two calculations.

Careful examination of Figure 6-10 will show that the downcomer flow rate becomes negative just before 1000 s. This indicates that flow in the downcomer has reversed. This graph shows only the net downcomer flow. The reversal trend starts around 960 s when flow in the cold-side downcomer (channels 4 and 6 in Figure 2-2) reverses. Between 960 s and 970 s the cold-side downcomer flow reverses back to the usual direction and the hot-side downcomer flow reverses. By 1000 s the net flow in the

downcomer channels is negative. It should be noted that when the flow in a downcomer channel reverses, there is no flow of liquid back up into the steam dome region. Rather, the liquid flows up the downcomer into the region surrounding the feedwater ring. It is here that the liquid from the reversed channel flows back down the other side, creating a downcomer recirculation loop. Now, the geometric model used by THERMIT-UTSG is suspect under these conditions, since the code allows flow between downcomer channels only at the bottom and the top (above the feedwater ring). The reversal of only some of the downcomer channels may not adequately describe the actual downcomer flow, since there can be azimuthal flow along the downcomer. However, the asymmetry in the evaporator/riser channels does provide a driving force for this behavior. Since the net flow becomes negative shortly after the initial reversal and the magnitude of the flow is relatively small, the model deficiency is probably not crucial to the remainder of the calculation. TRAC also predicted downcomer flow reversal but at a later time (~1190 s).

The sharp reduction in outlet steam flow with only a gradual decrease in MFW immediately after turbine trip causes a substantial accumulation of water in the system. Figure 6-12 shows that the water inventory increases by almost 11,000 kg. TRAC predicted an increase of nearly 20,000 kg. Since there was substantial disagreement in this quantity before scram, the different increases are not surprising. However, the trends predicted by the two codes are nearly the same until very late in the transient. The increase in water inventory does not necessarily mean that the downcomer water level increases. In fact, immediately following scram, the water level falls (see Figure 6-13).

This is simply a redistribution of the water inventory within the system. The lower heat transfer rate implies that boiling will occur higher in the evaporator, increasing the volume of the single-phase liquid region at the bottom. The increase in water inventory continues until the MFW flow drops below the outlet steam flow. Then, some of the increased inventory is boiled off. As the rupture flow continues, the steam generator slowly fills, producing an increase in both downcomer level and water inventory.

Figure 6-14 shows how the boiling front changes with time. Following scram, the boiling front begins to rise in the evaporator due to the lower power. Also, note that the top of the evaporator/riser begins to boil dry. In fact, the steam in this region is slightly superheated until 1700 s. The axial void distribution in the evaporator/riser becomes much steeper as the length of the two-phase region decreases (see Figures 6-16 to 6-20).

As the flow through the evaporator/riser channels decreases, the interfacial drag on the liquid becomes insufficient to overcome the gravitational force. There is an increasing amount of liquid fall-back as the flow approaches stagnation. This behavior is asymmetric with fall-back occurring primarily in the hot channel. There is significant crossflow from the hot to cold channel in the evaporator and from the cold to hot channel in the riser. This sets up a kind of liquid internal circulation loop, which acts to increase the exit void fraction. However, as the flow stagnates in the evaporator/riser, this asymmetry essentially disappears.

Surprisingly, the boiling front calculated by TRAC (Figure 6-15) is nearly stationary (except for a brief rise before 1000 s) for several

minutes after scram. Figures 6-17 and 6-18 show that the evaporator/riser void is much lower than that predicted by THERMIT during this period. The steam does not boil dry in the riser as predicted by THERMIT.

After the substantial changes caused by reactor scram and turbine trip, the secondary-side thermal-hydraulic conditions in comparison change slowly. The steam flow out the ADVs and SRVs gradually falls off as the pressure build-up following turbine trip is relieved (see Figure 6-9). There is a momentary cessation of the steam flow near 1200 s. Here, the operator closes the ADVs. A small pressure increase following this action causes the SRVs to lift, and there is a small steam flow until 1590 s. After this point the SRVs are essentially closed.

Because the THERMIT and TRAC models respond differently, the steam dome pressure boundary condition, taken from the TRAC calculation, will not in general produce a steam flow that is identically or even nearly zero after 1590 s. In fact, THERMIT calculated a negative steam flow (from the steam line into the steam dome) for the given steam dome pressure. This does not correspond to reality, since by this time the operator has isolated the damaged steam generator. This is a fundamental problem of running a component simulation code with boundary conditions taken from a system code with a different model of the component. To prevent this nonphysical situation we switched to a zero steam flow boundary condition at 1600 s. After this time, the steam dome pressure is calculated in place of the steam flow rate. Figure 6-21 shows how the steam dome pressure drops after 1600 s. The difference between the THERMIT and TRAC values is an indicator of the cumulative difference in the response of the two models. Even with the

zero steam flow condition, the situation is still not physically realistic because there is no feedback of this reduced pressure to the other boundary conditions -- particularly the rupture flow rate. A lower secondary-side pressure would produce a larger leakage rate and also extend the time at which the leakage could be controlled. Since this would prolong the accident longer than predicted by THERMIT (or TRAC), this observation is important.

Figures 6-10 and 6-11 show that the TRAC downcomer and riser flows remain high for more than 200 s after the MFW is shut off. After 1200 s there are substantial oscillations in the flow and many reversals in both downcomer and the riser. The flow spike in the riser after 1200 s appears to be unreasonably large for the situation at this time in the transient. By comparison, the downcomer and riser flows in THERMIT are reasonably constant after 1000 s. We suspect that oscillations of the magnitude given by TRAC indicate a hydrodynamically underdamped steam generator model. During times of flow reversal, TRAC predicted flow from the downcomer back up into the steam down and down into the riser. Now, because the steam dome pressure is usually lower than in the rest of the steam generator during these oscillations, there is significant flashing as the flow enters the steam dome. However, the steam dome model does not completely remove all the vapor flow, as noted previously, and hence substantial flow was returned to the riser where much of the steam condensed. The large flow oscillations and the reversed flow through the steam dome are questionable. Further examination of this behavior is warranted.

After scram, THERMIT predicted a gradual narrowing of the two-phase region in the evaporator/riser channel (see Figure 6-14). By 1600 s a

relatively sharp vapor-liquid interface had formed midway up the channels. The axial void distribution after this time was very steep as Figures 6-19 and 6-20 indicate. The evaporator/riser conditions predicted by TRAC were quite different. The boiling front before 1540 s was nearly stationary with low void throughout the evaporator/riser. At 1540 s the void suddenly collapsed and the boiling front moved well up into the riser. (Actually, it was flashing not boiling that occurred in this region, since the boiling front was above the tube bundle.) The mechanism for this sudden collapse is unknown. A more gradual change would seem more physical for the given power behavior.

The two codes also predicted very different times for heat transfer reversal. This occurs when the primary fluid temperature drops below fluid temperature in the evaporator, and there is heat transfer from the secondary side to the primary side. TRAC predicted this to occur at 1590 s; THERMIT predicted it to occur at 2140 s.

The THERMIT calculation took 54,098 time steps requiring 7820 s of CPU time on a CRAY-1 computer. We found two things that were responsible for the high CPU time used by the code. The heat transfer calculation and the recirculation model calculations are performed explicitly. In an explicit calculation the timescale characteristic of the process limits the time step that can be taken without numerical instabilities. Unfortunately, the code only checks the convective limit to control the time step. Because of instabilities observed in the heat transfer and recirculation model calculations, we found it necessary to reduce the maximum time step permitted during several periods of the calculation. This greatly increased the computational time of code.

VI.2 Modified Case 1

This scenario was a modified version of the base case calculation performed at LANL. The principal difference between this scenario and Case 3 is that all of the reactor coolant pumps trip on low primary pressure instead of just two of the four. The particular scenario that we ran differs from that described in Reference 1 in that the main feedwater (MFW) was not entirely shut off following scram but reduced to 5% of full flow. In addition, the auxiliary feedwater (AFW) was turned on at a rate of about 3% of full flow. The AFW is very cold (277.6 K). Until scram this run was identical with that of Case 3.

We experienced severe computational problems with this calculation about one minute after scram that led to code failure. The problems resulted from the method that THERMIT-UTSG uses to set the downcomer boundary conditions. The temperatures and pressures in the downcomer mesh cells above the feedwater ring (or the water level if it is below the feedwater ring) are set by the recirculation model to give the correct flow and enthalpy resulting from the mixing of the recirculation flow and the feedwater flow. This method works satisfactorily under normal flow conditions. However, it experiences some difficulty during periods of flow reversal. The very cold AFW makes the problem more severe because of the large temperature difference between it and the recirculation flow. The code was able to handle these conditions when the time step was reduced. Unfortunately, another complication occurred at this time. The downcomer water level fell below the feedwater ring. When this happens, the code begins to mix the feedwater with the vapor. Because of the presence of the cold AFW, this is a very severe phenomenon. All attempts at gradually apportioning the feed flow

between the vapor and the liquid regions failed since the water level dropped very rapidly during this part of the calculation.

The code failed because of unrealistic thermodynamic conditions that were calculated in the upper downcomer. Capability to calculate such transients in the future would require changing the method used by the code to set the downcomer boundary conditions.

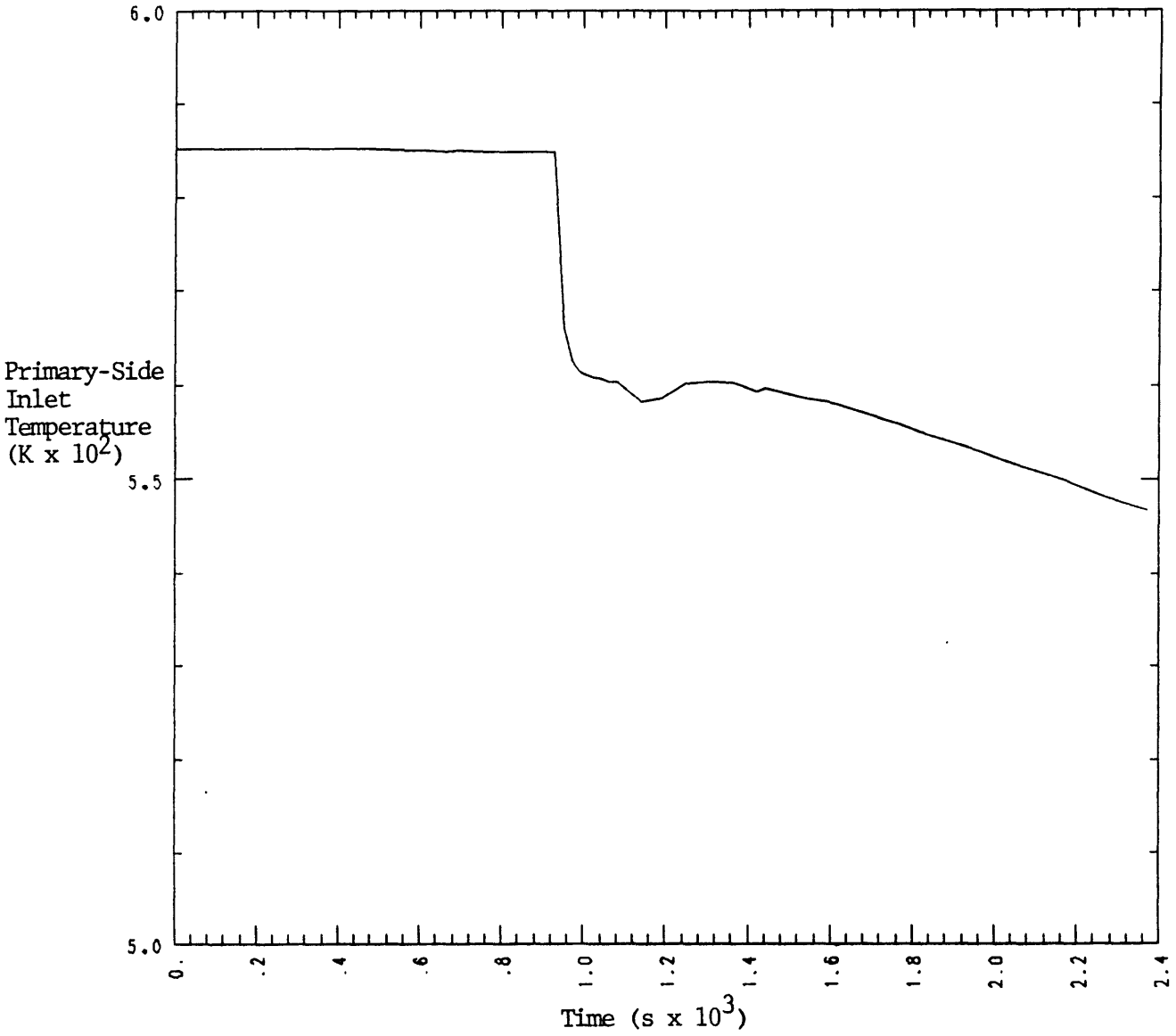

Fig. 6-1. Primary-Side Inlet Temperature

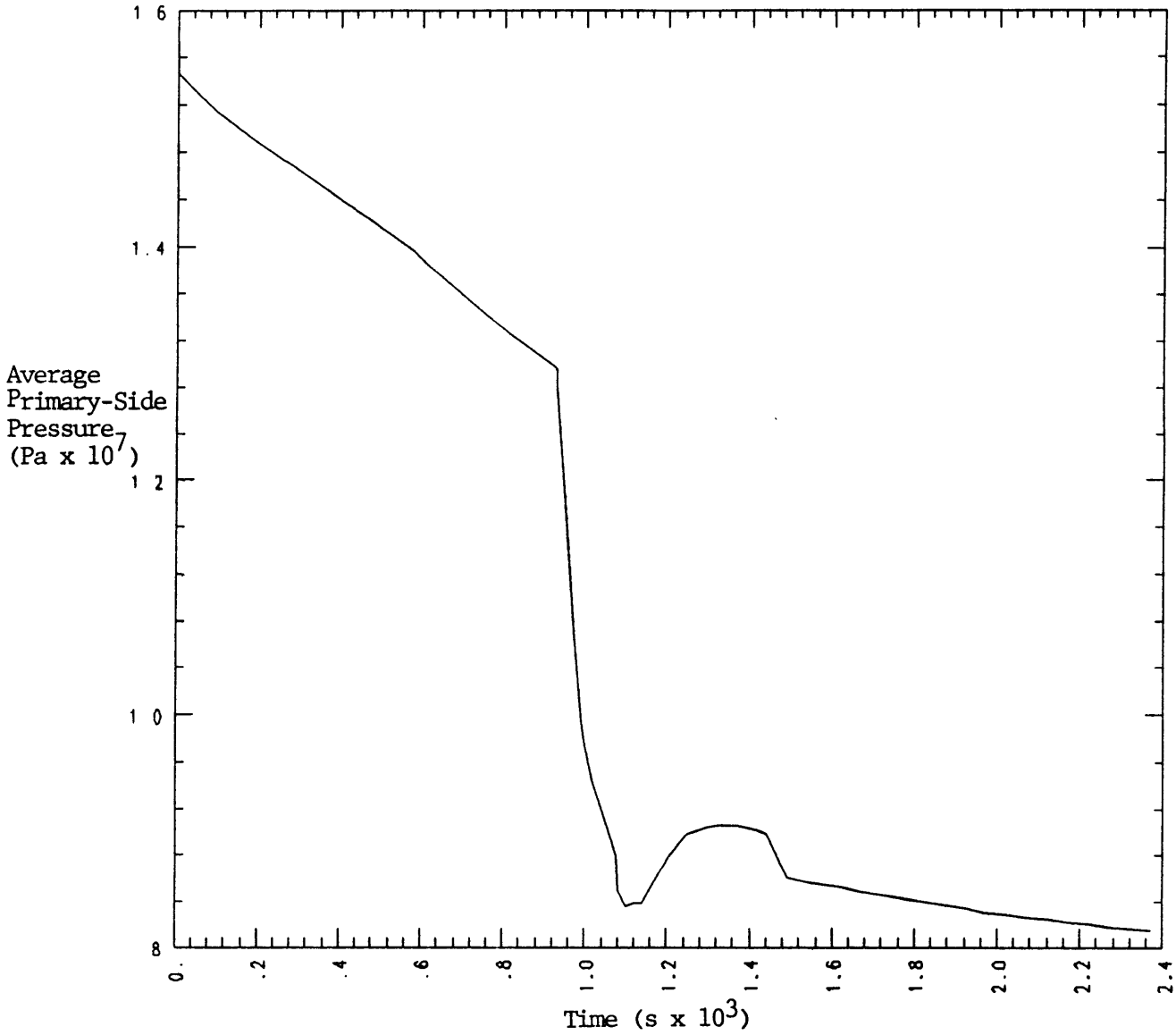

Fig. 6-2. Average Primary-Side Pressure

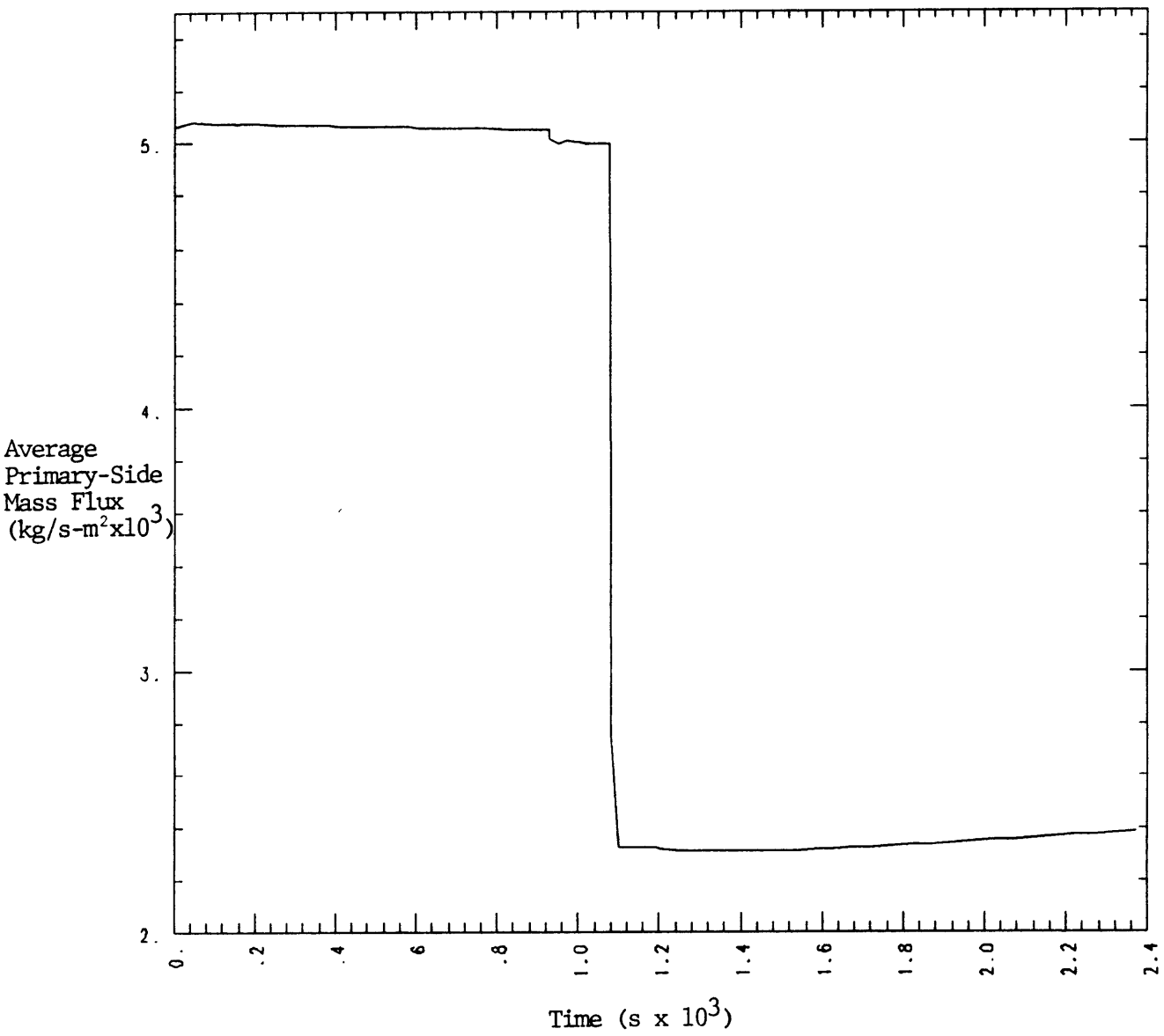

Fig. 6-3. Average Primary-Side Mass Flux

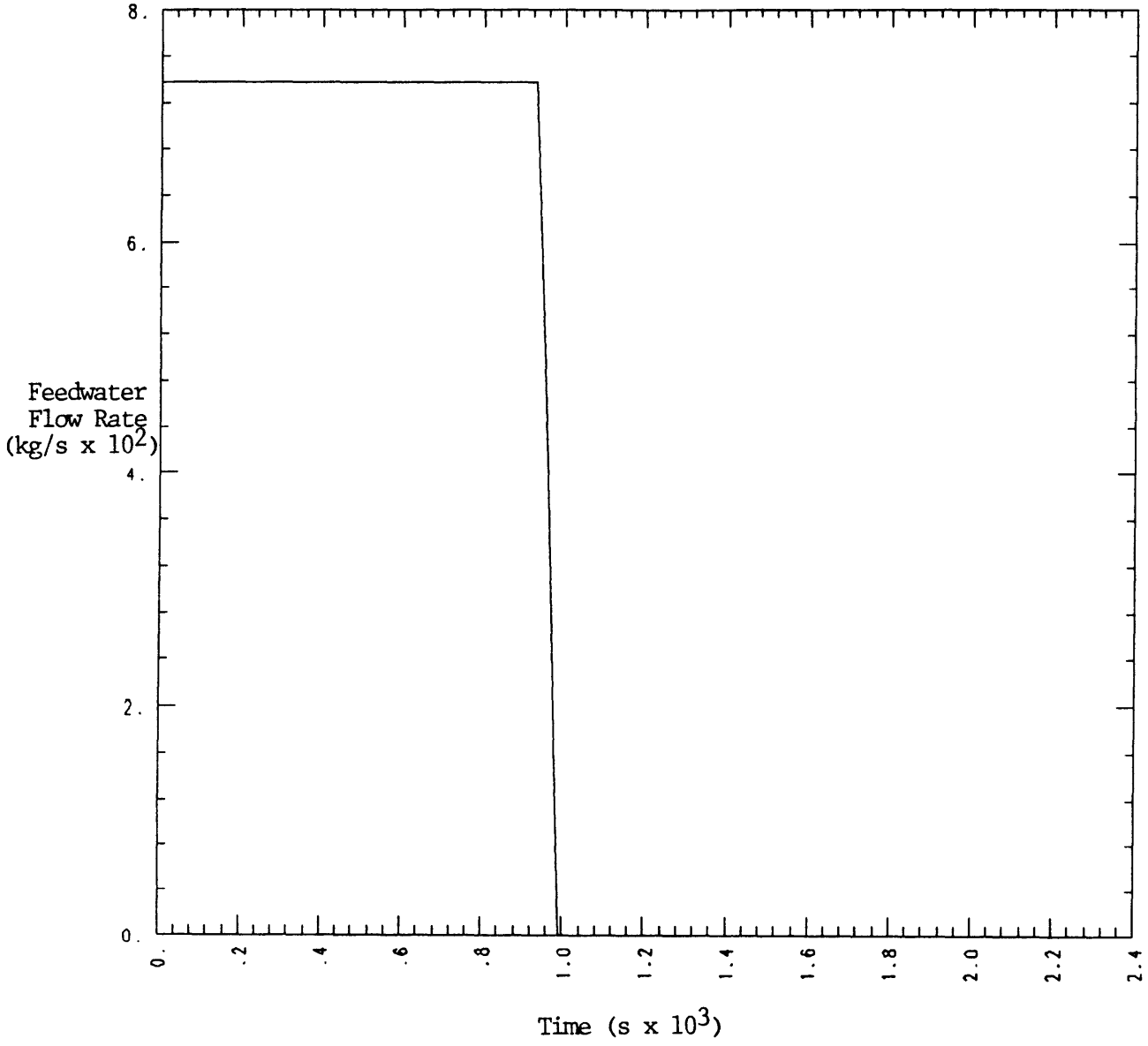

Fig. 6-4 Feedwater Flow Rate

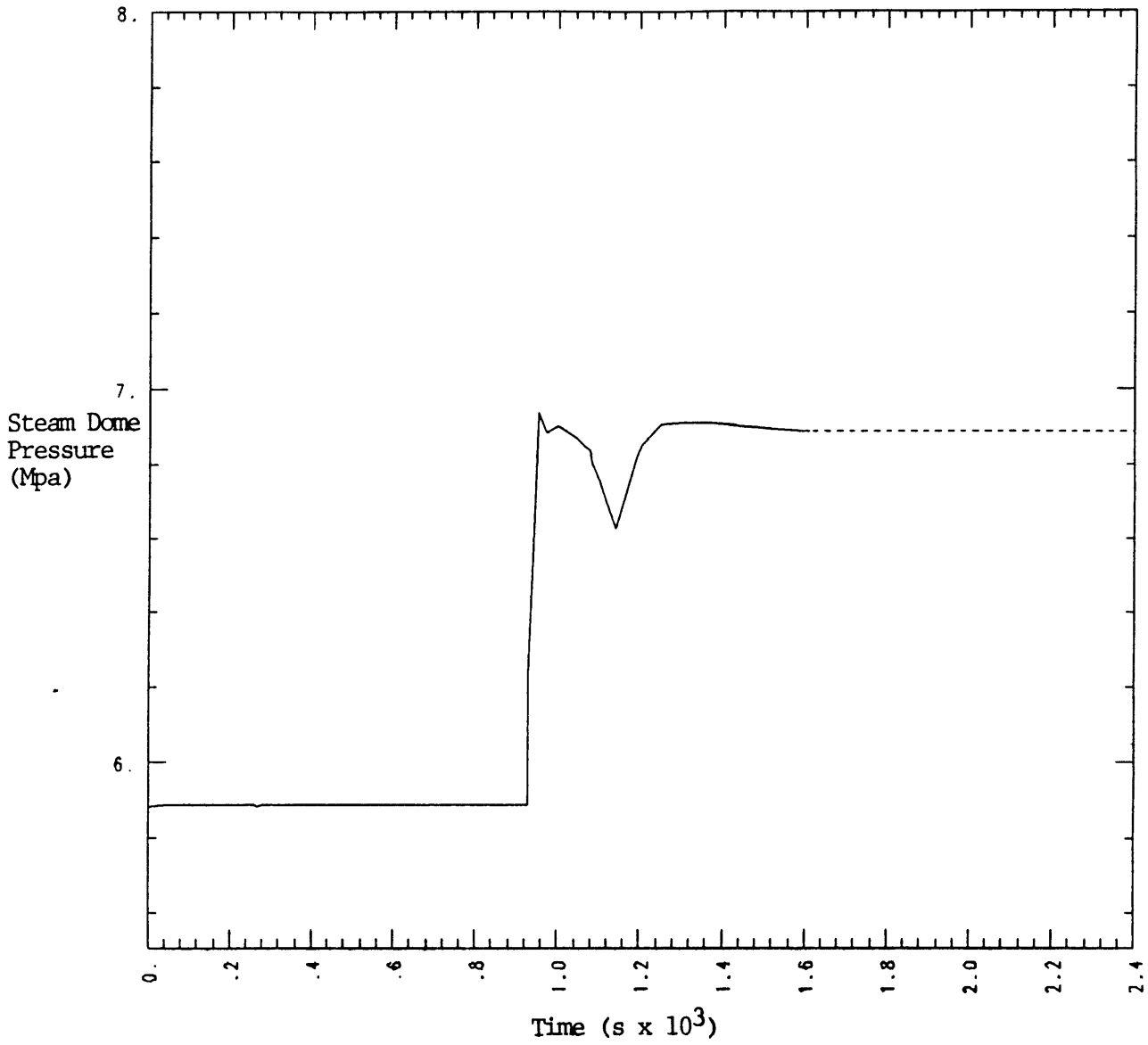

Fig. 6-5. Steam Dome Pressure

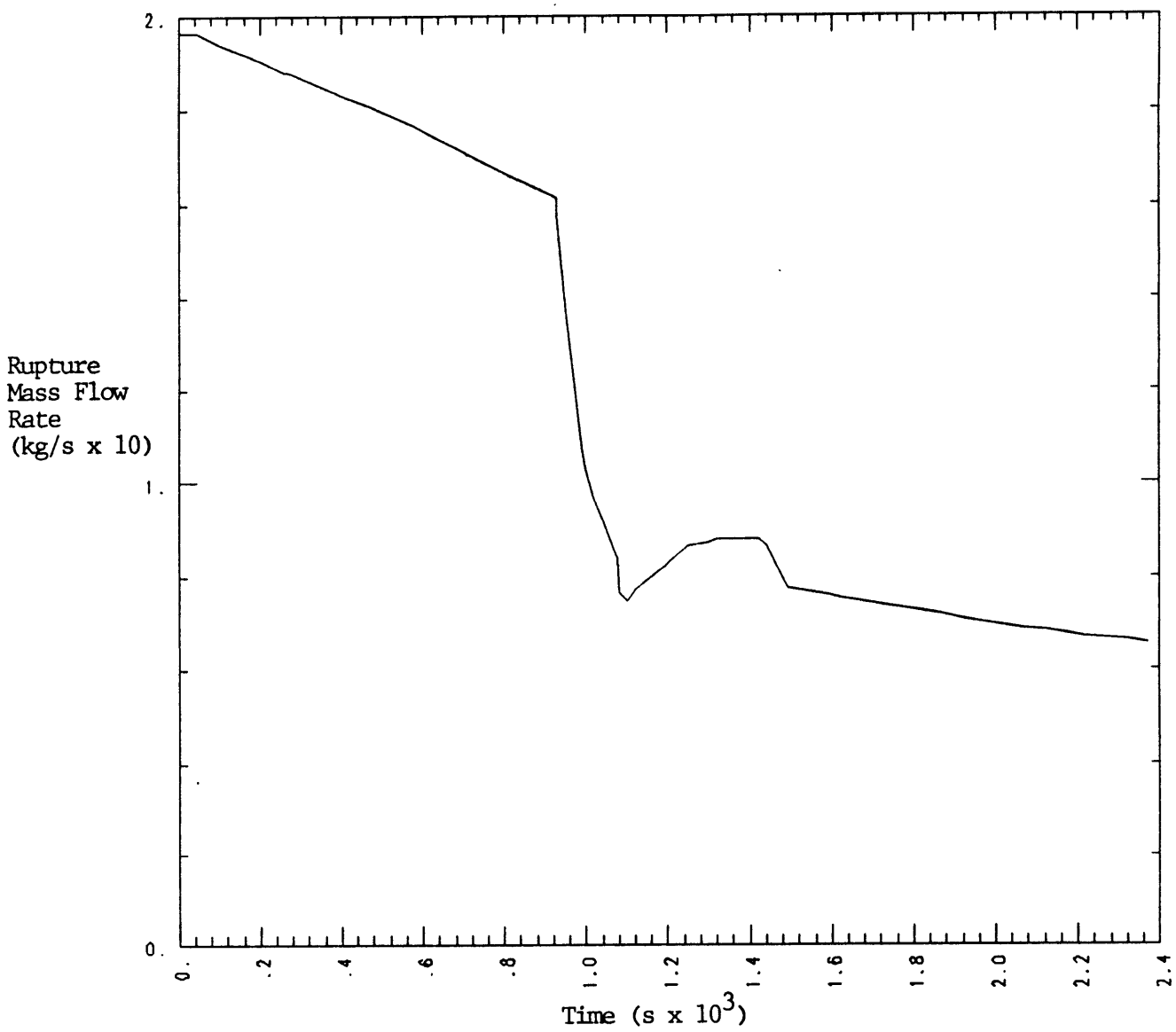

Fig. 6-6. Rupture Mass Flow Rate

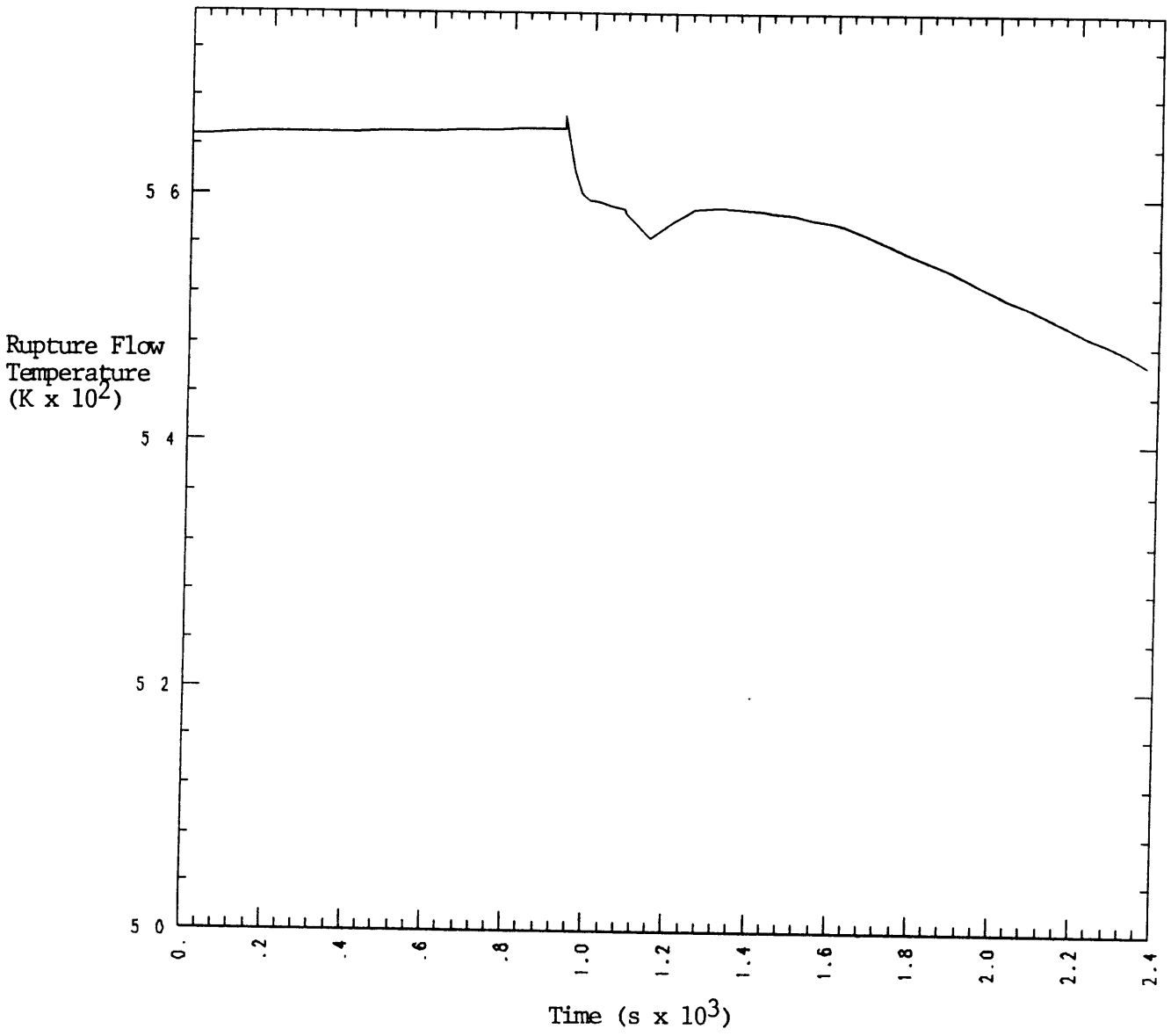

Fig. 6-7. Rupture Flow Temperature

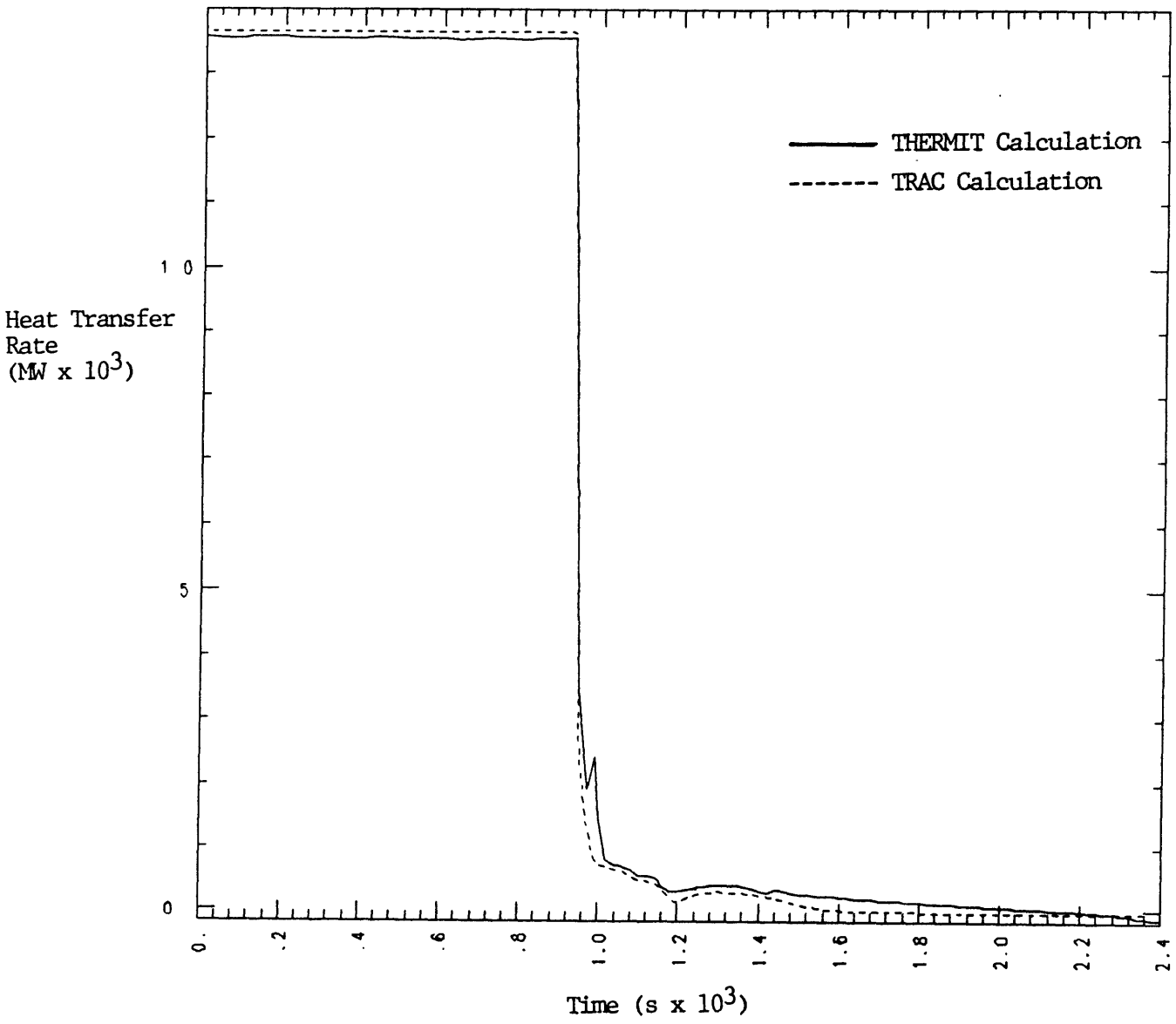

Fig. 6-8. Steam Generator Heat Transfer Rate

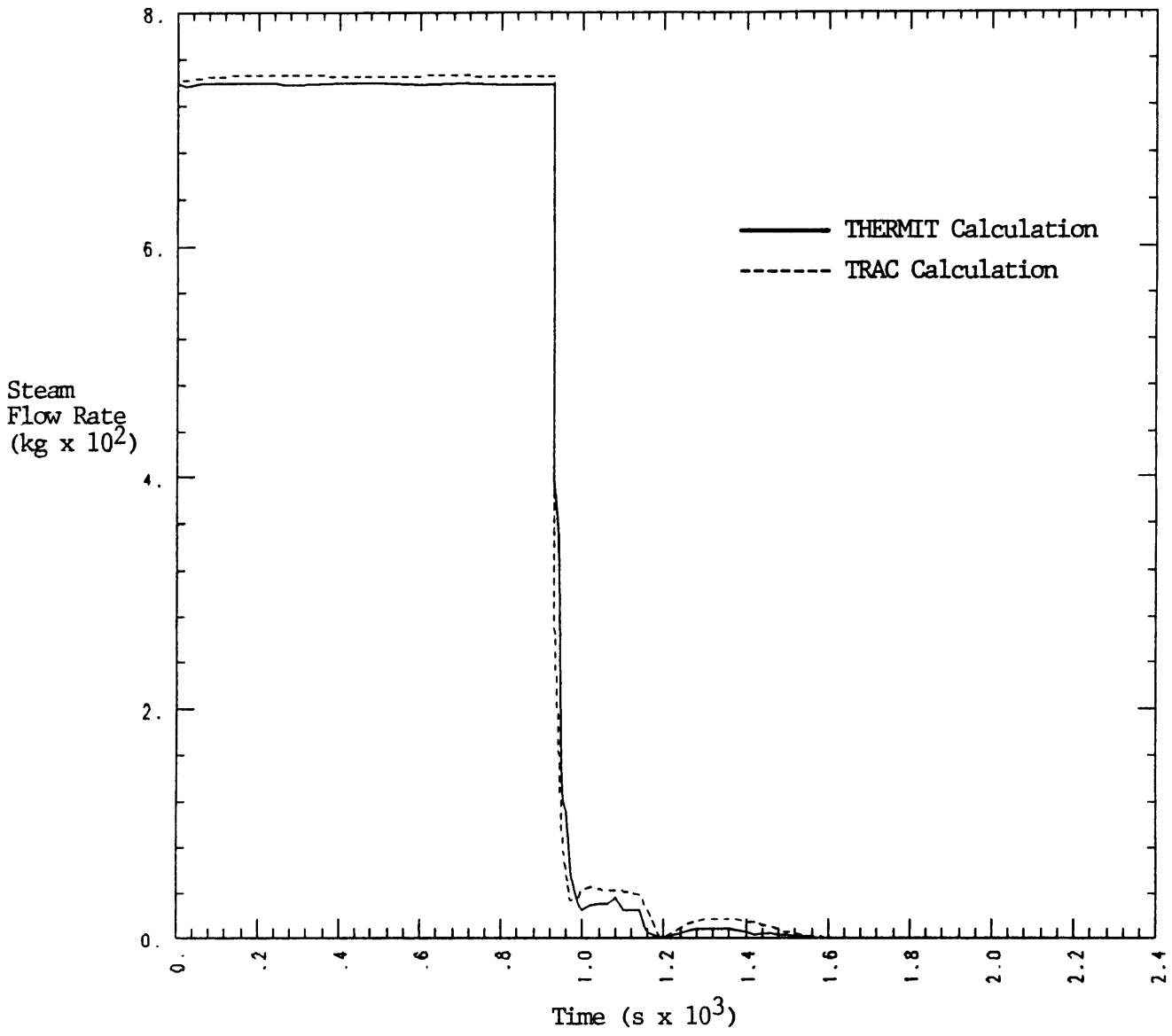

Fig. 6-9. Steam Flow Rate

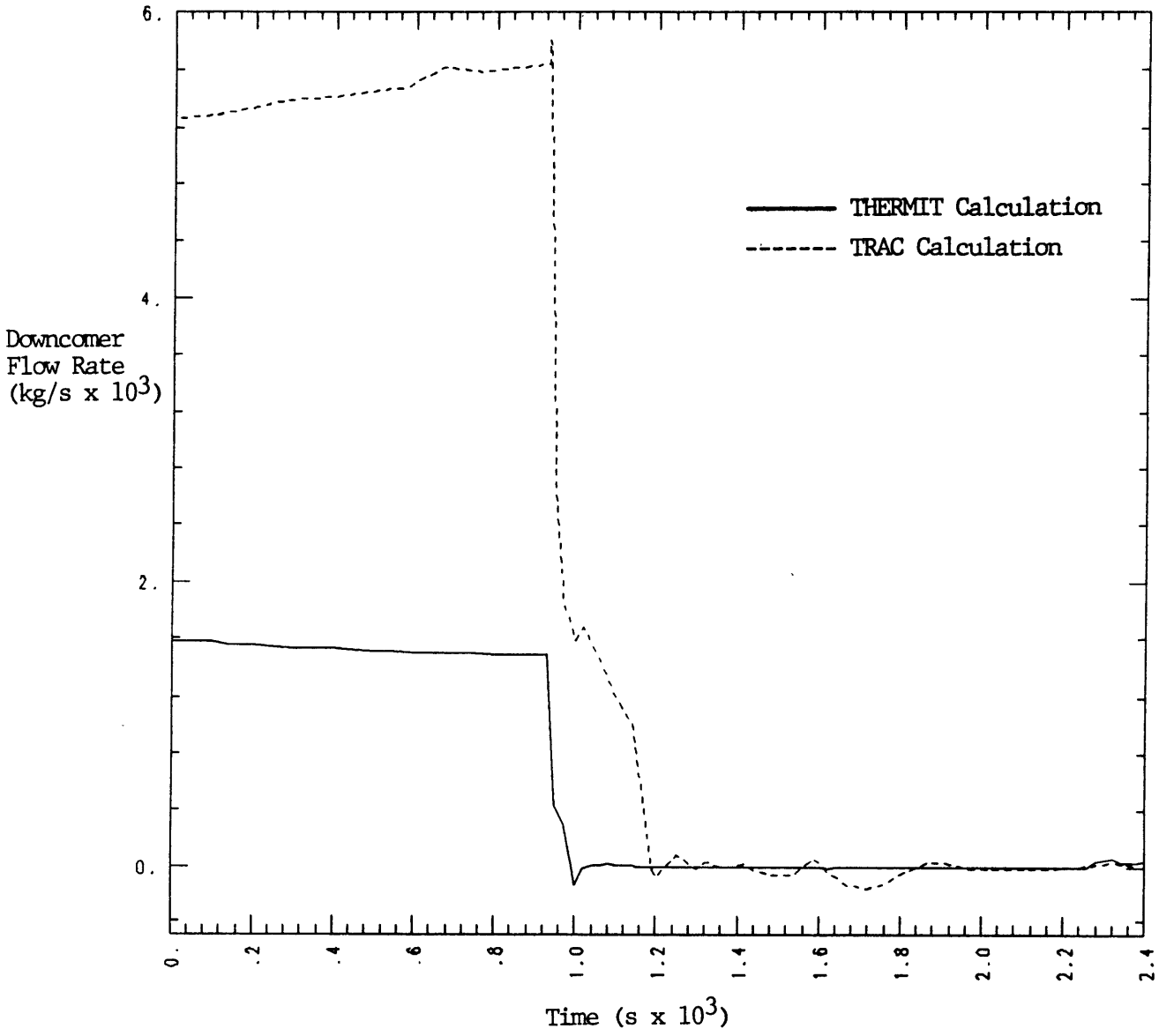

Fig. 6-10. Downcomer Flow Rate

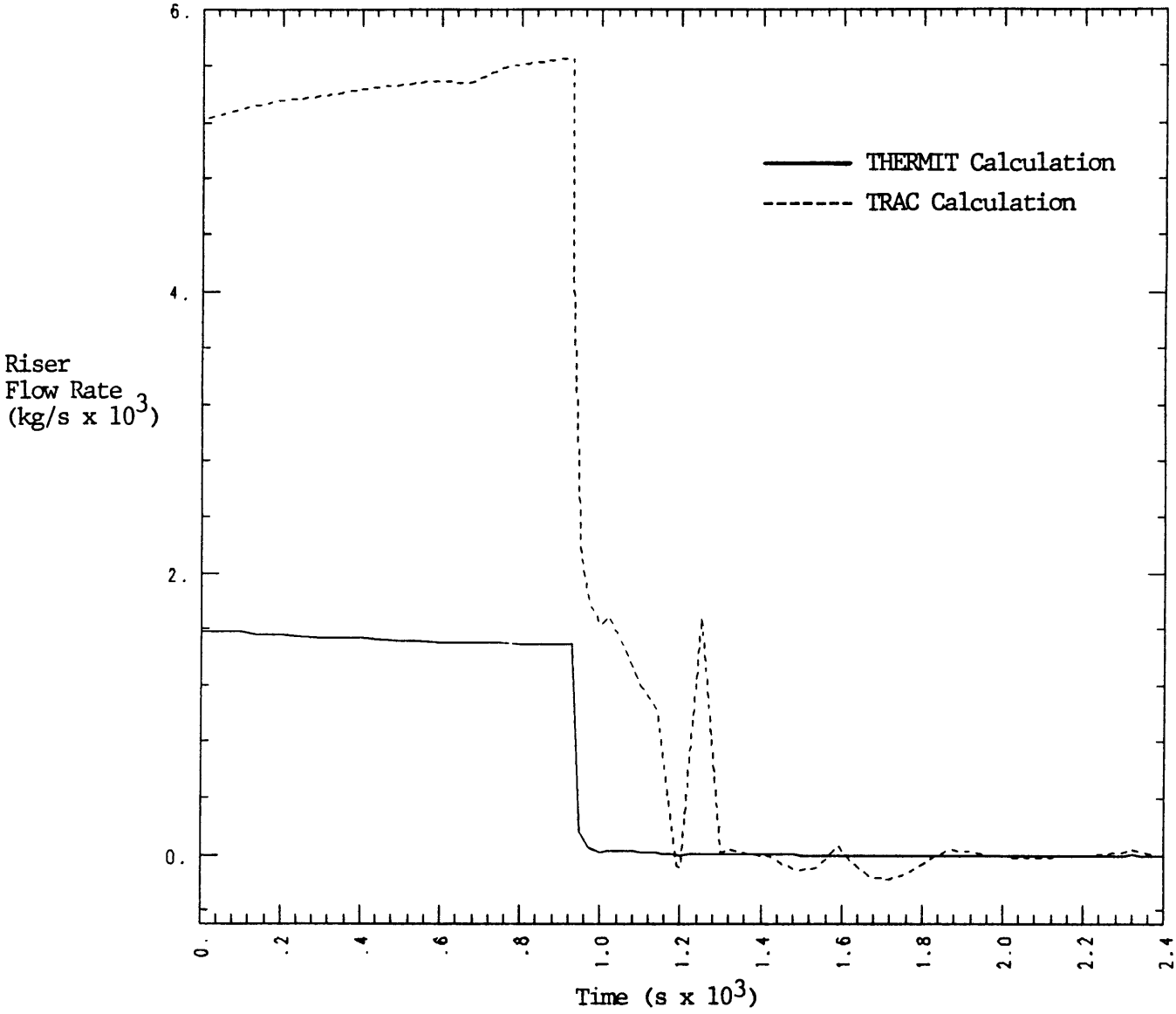

Fig. 6-11. Riser Flow Rate

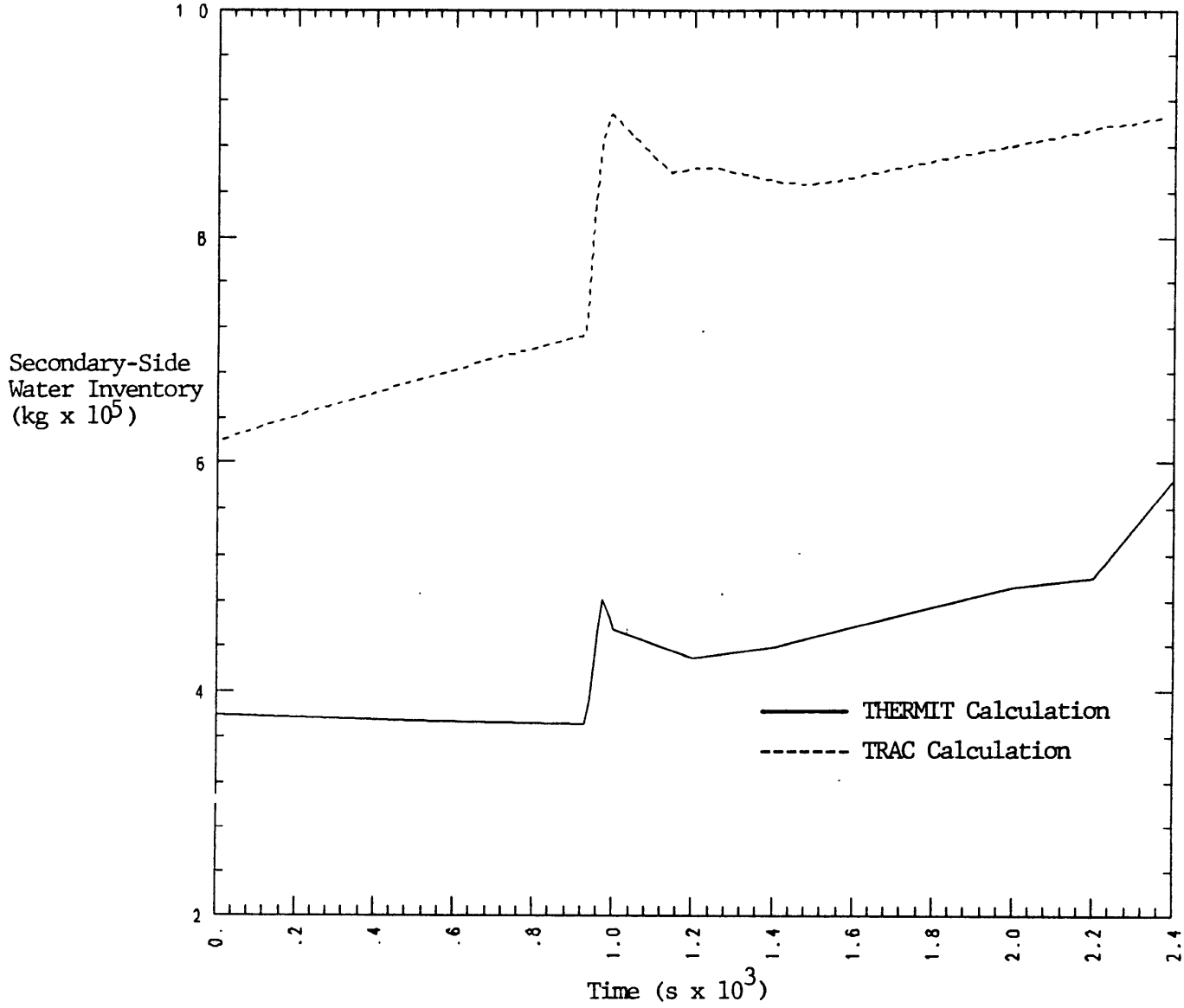

Fig. 6-12. Secondary-Side Water Inventory

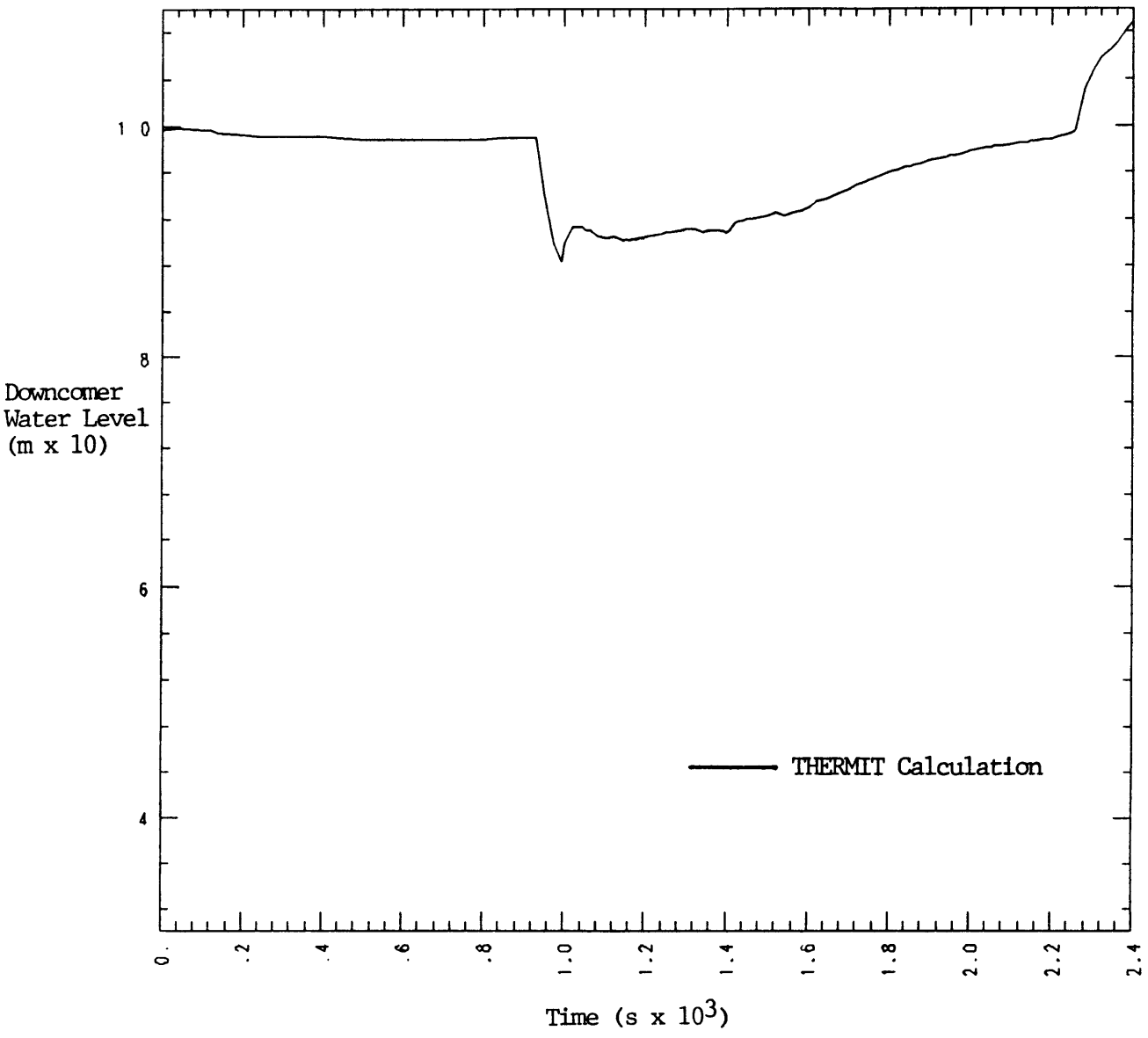

Fig. 6-13. Downcomer Water Level

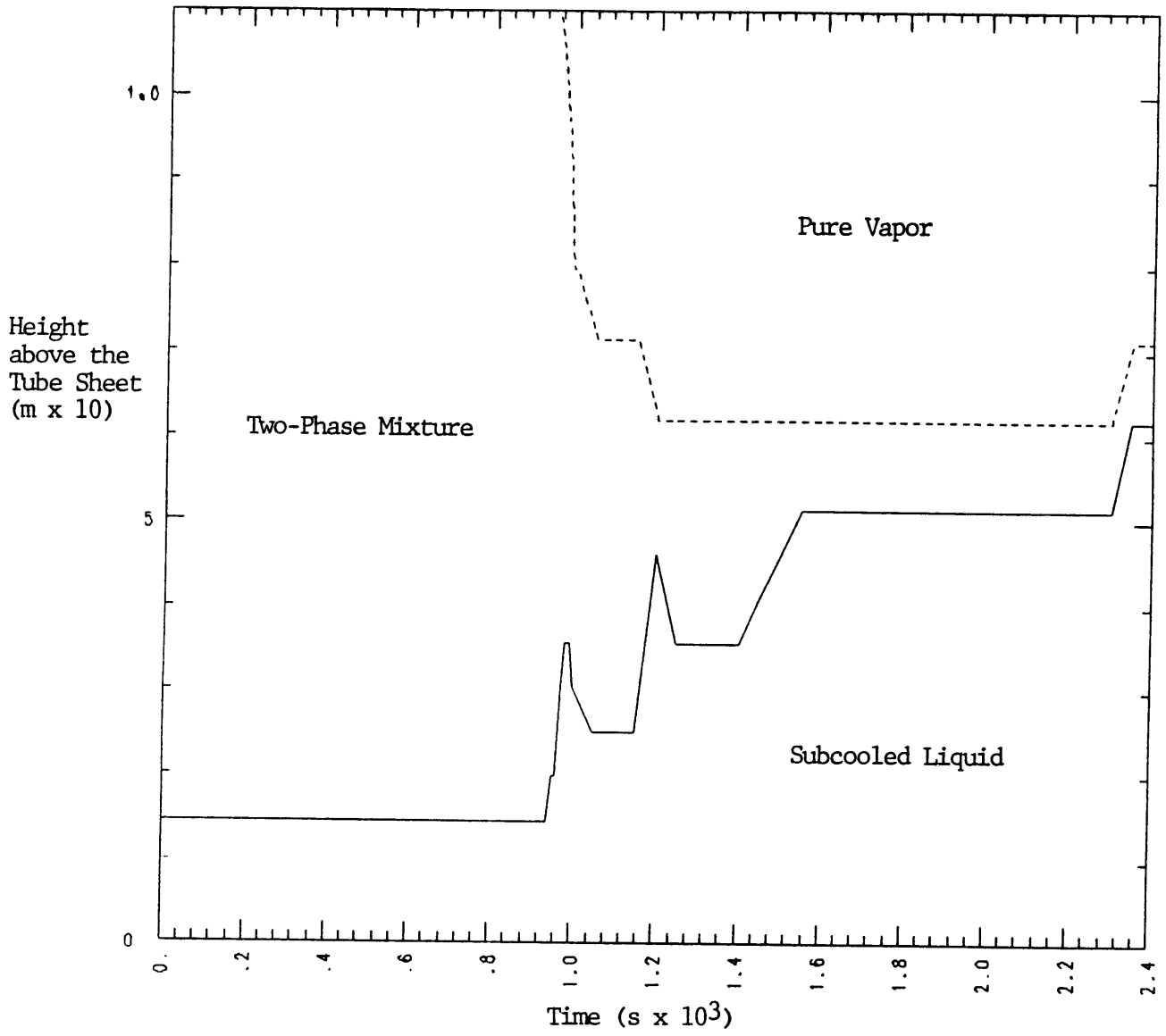

Fig. 6-14. Length of Two-Phase Region in the Evaporator/Riser: THERMIT Calculation

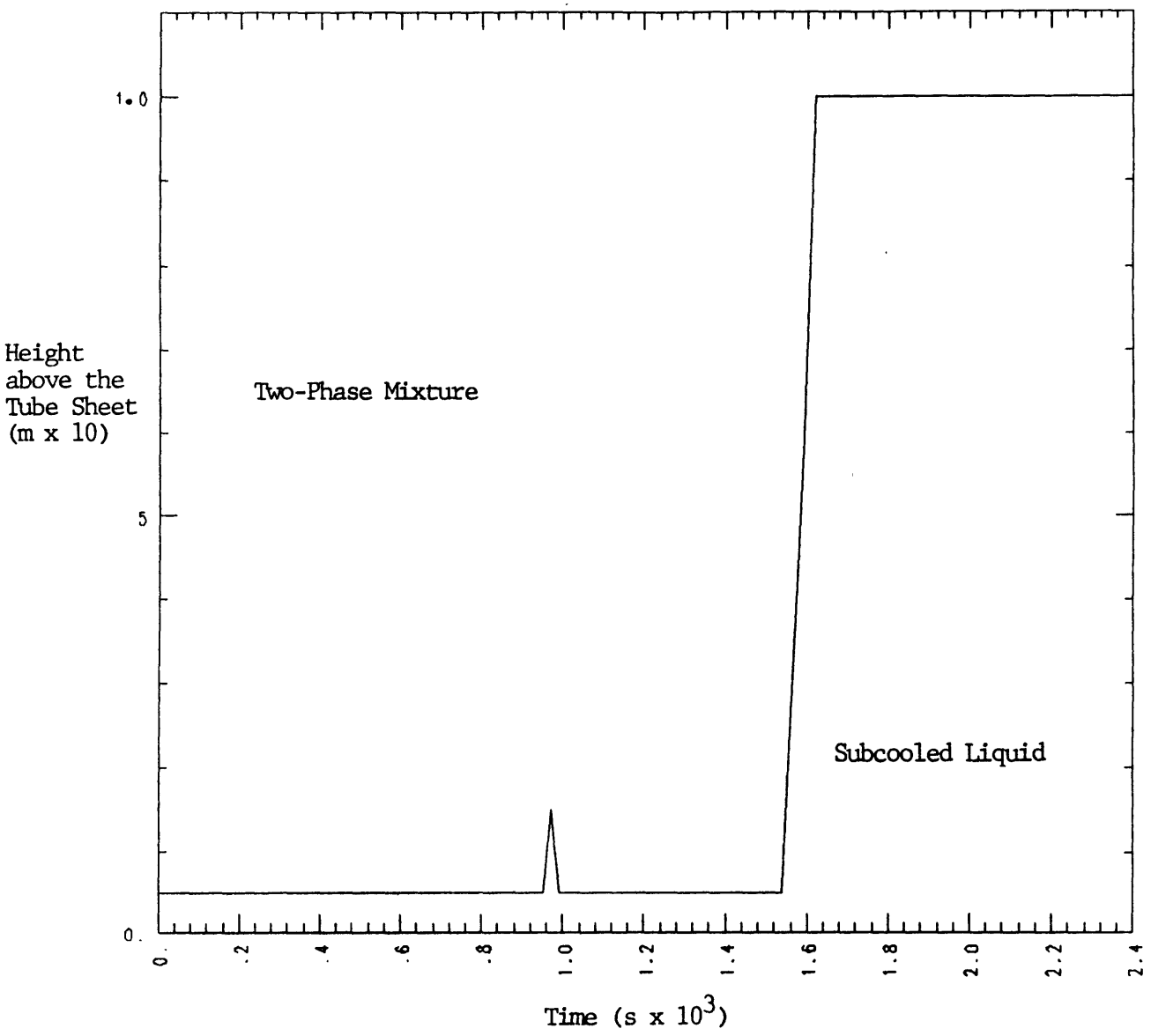

Fig. 6-15. Length of Two-Phase Region in the Evaporator/Riser: TRAC Calculation

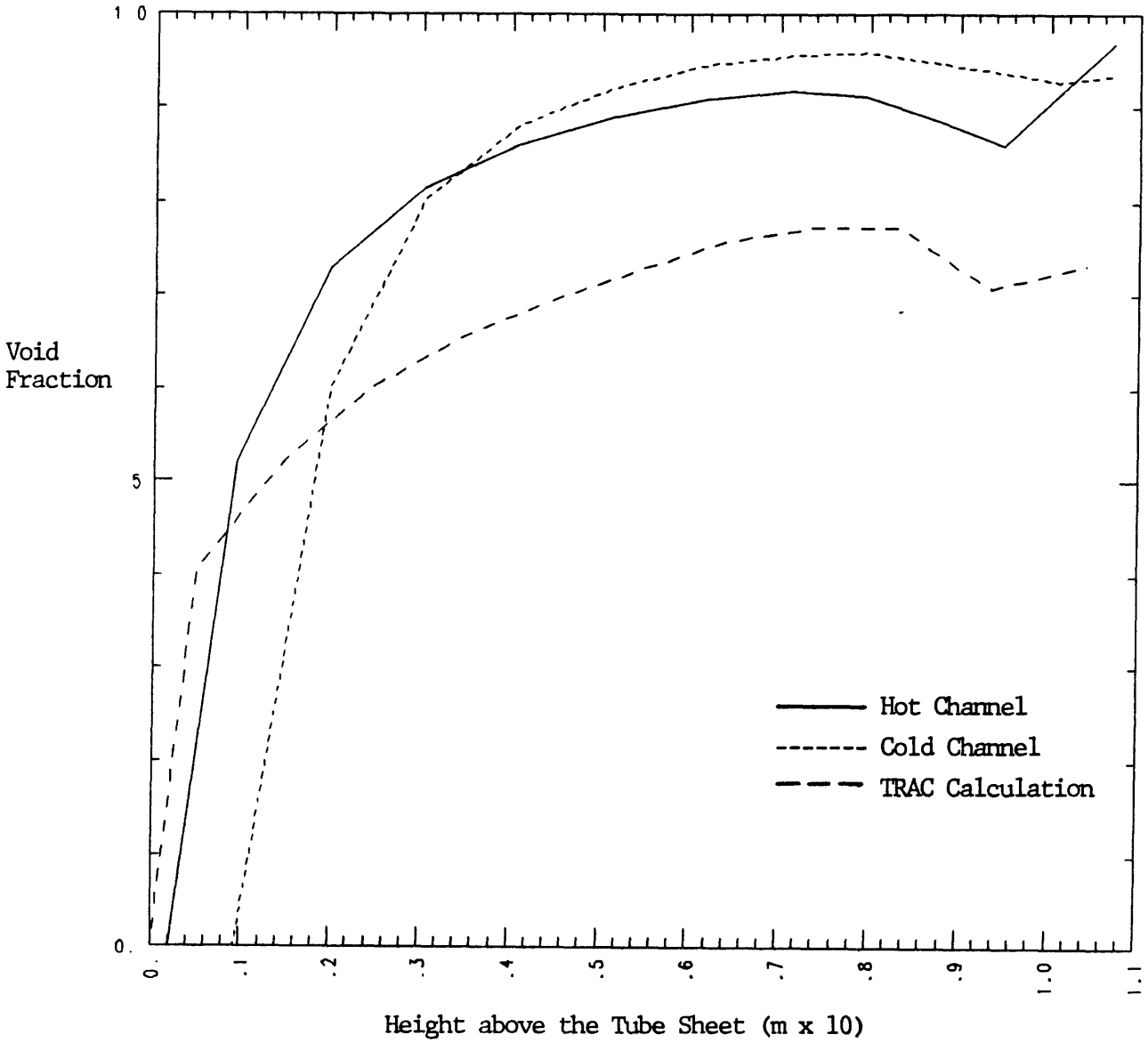

Fig. 6-16. Evaporator/Riser Void Fraction Distribution: 928 s

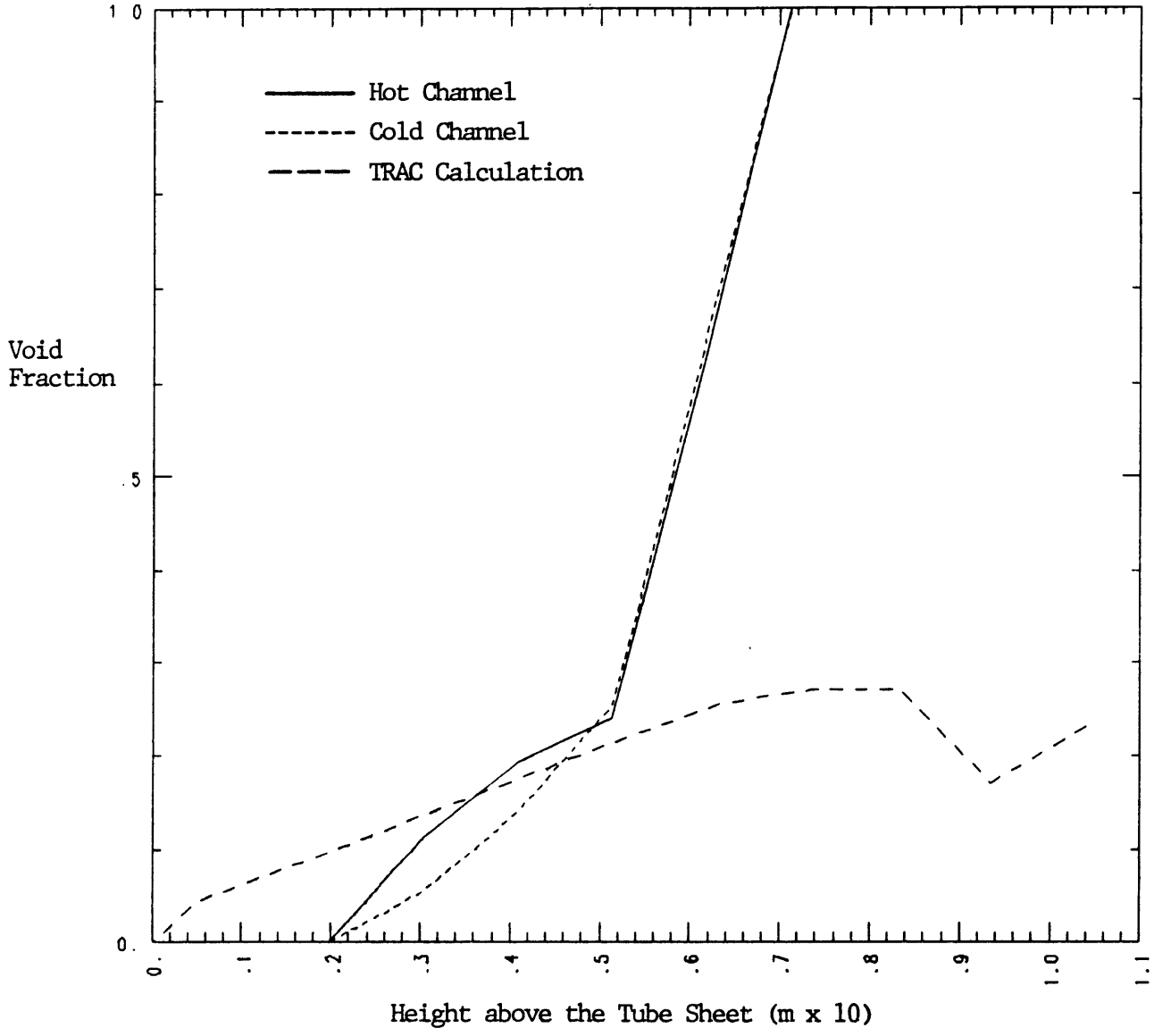

Fig. 6-17. Evaporator/Riser Void Fraction Distribution: 1000 s

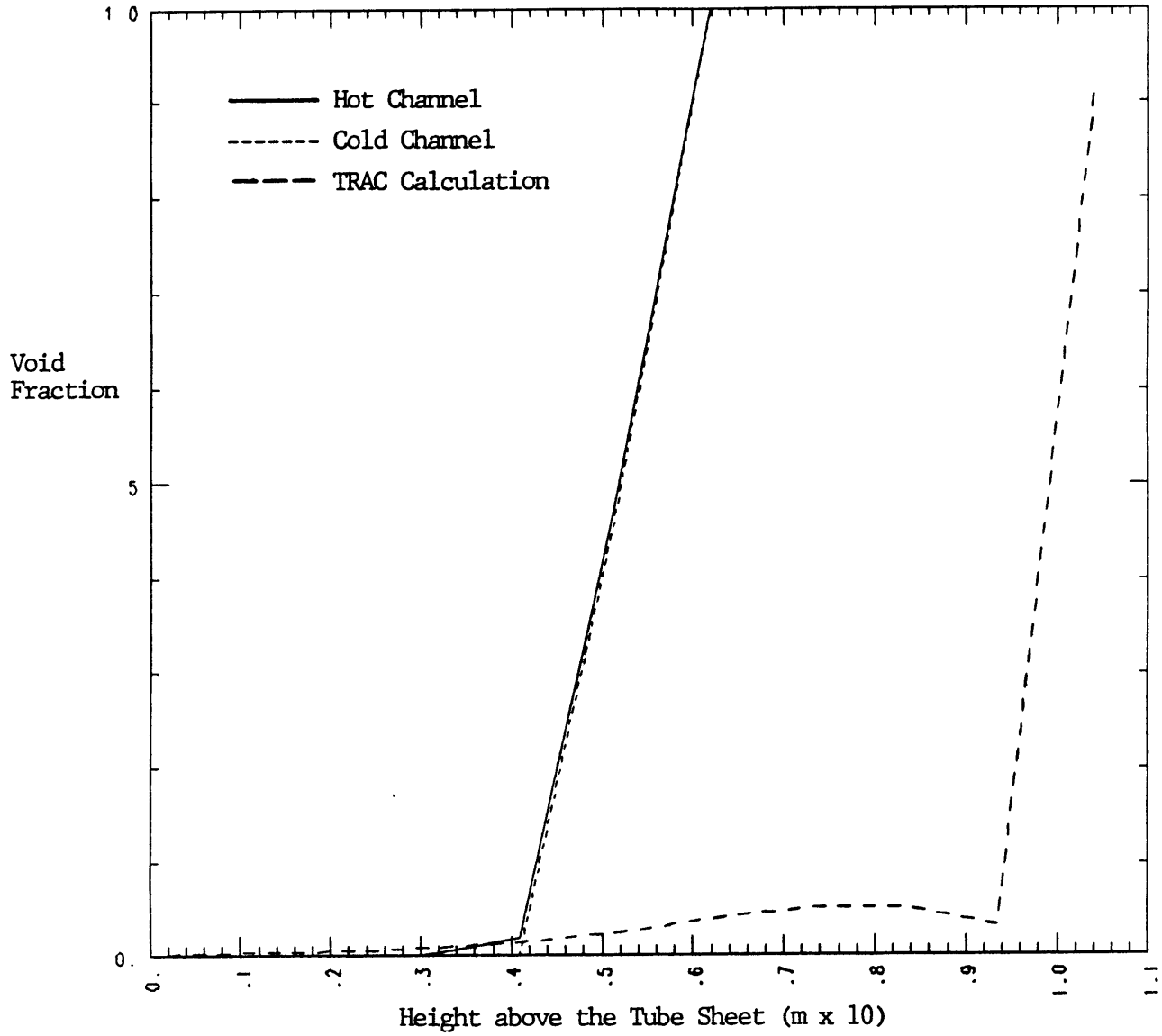

Fig. 6-18. Evaporator/Riser Void Fraction Distribution: 1200s

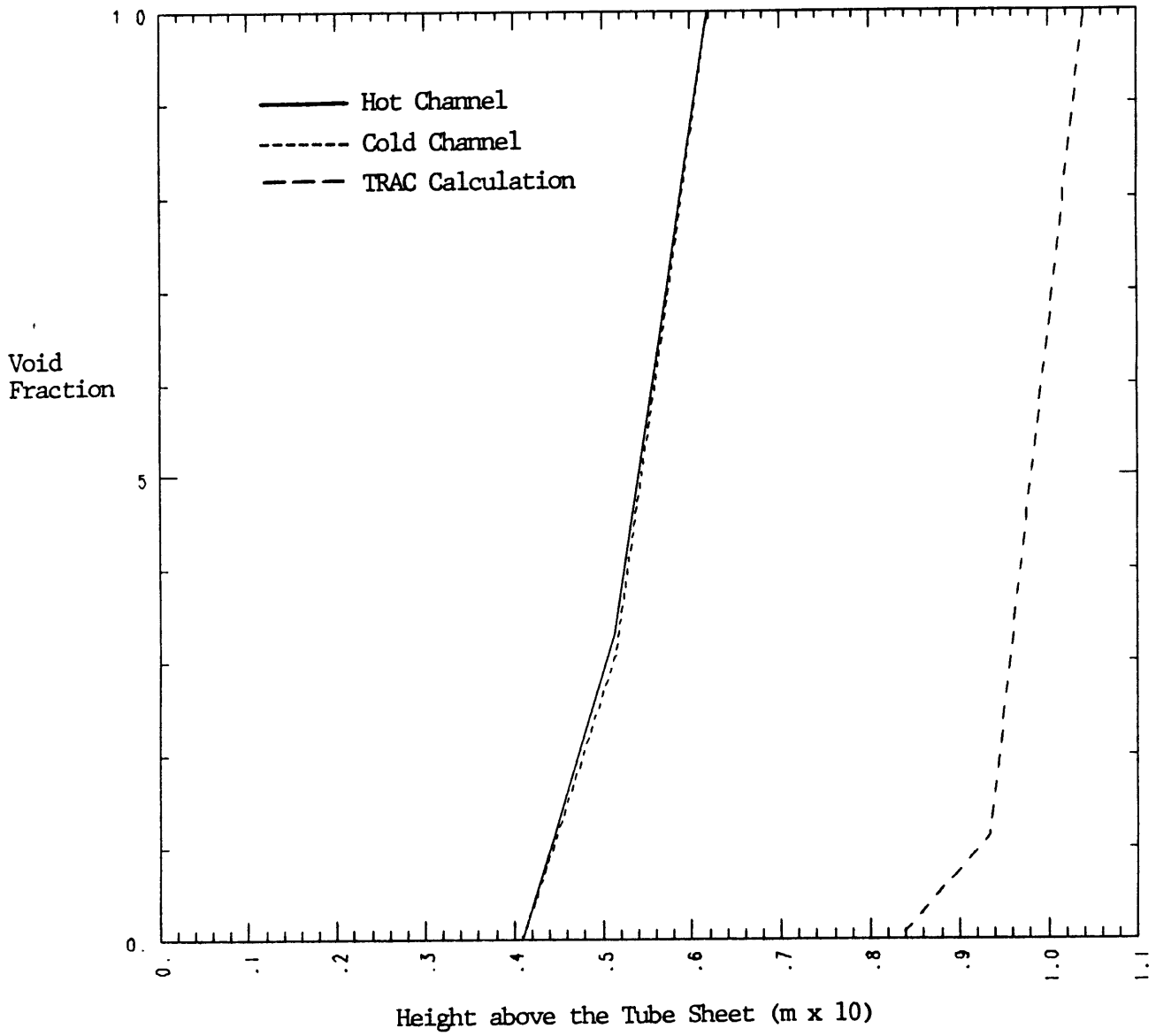

Fig. 6-19. Evaporator/Riser Void Fraction Distribution: 1700 s

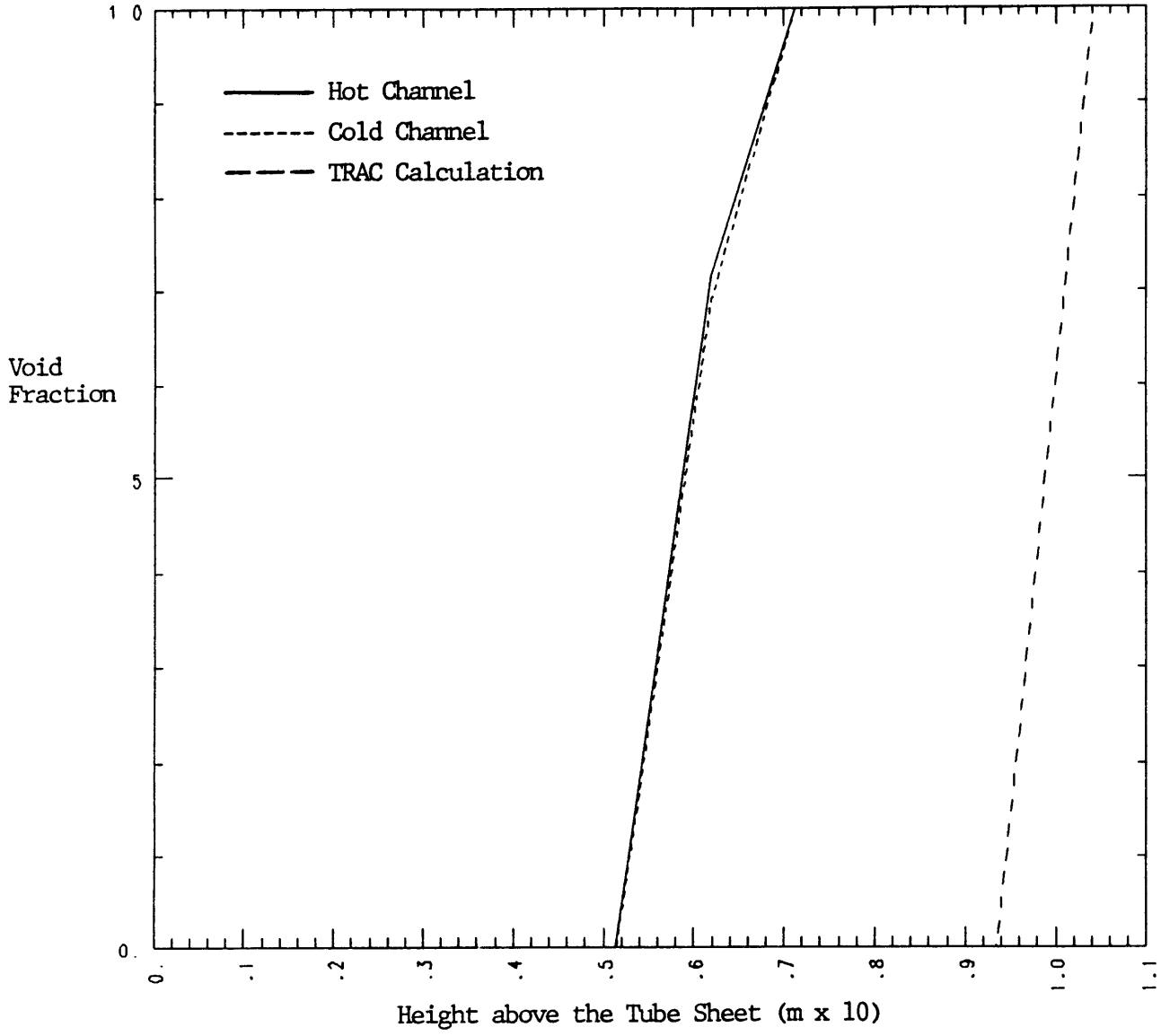

Fig. 6-20. Evaporator/Riser Void Fraction Distribution: 2400 s

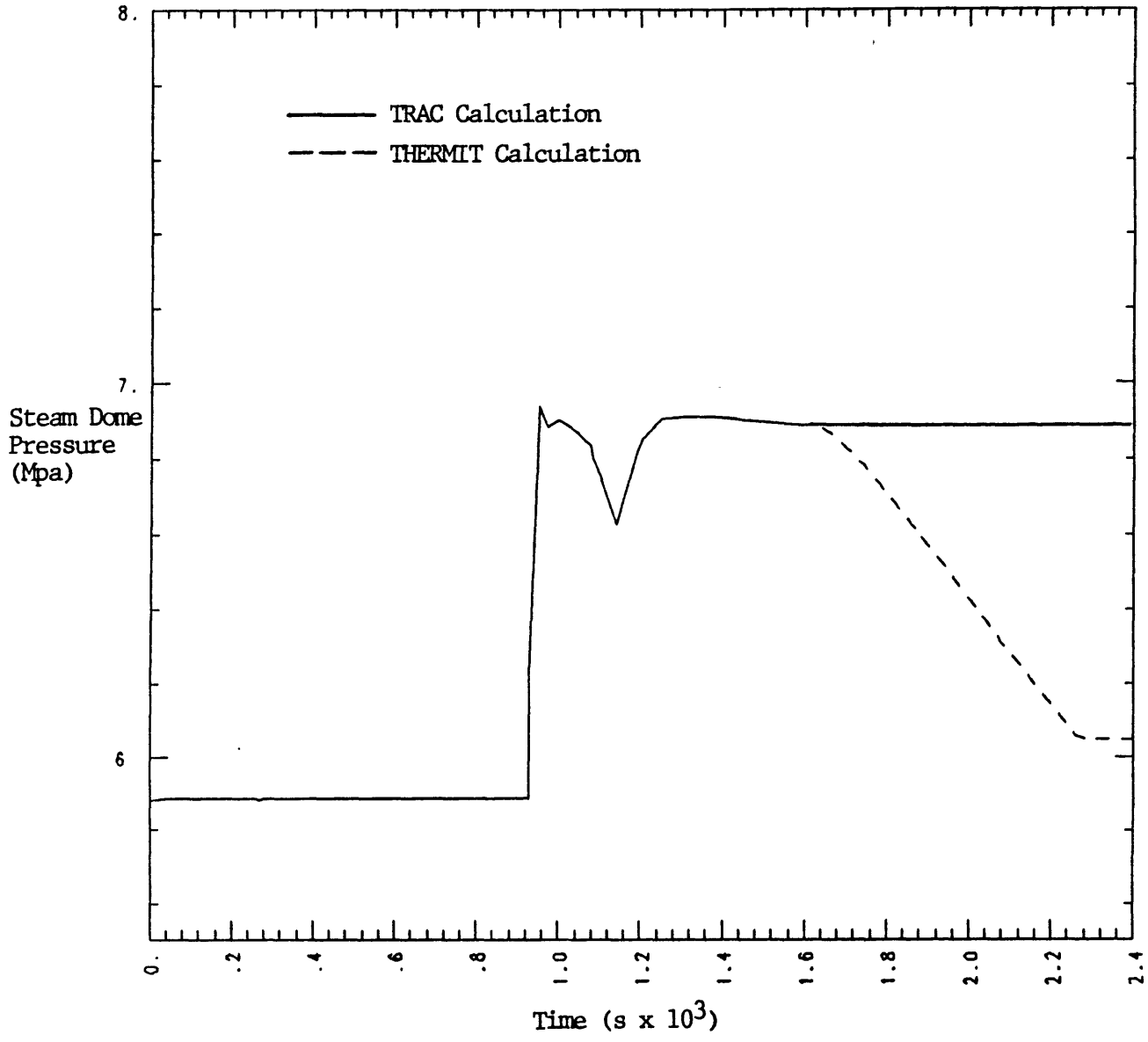

Fig. 6-21. Steam Dome Pressure

VII. Conclusions

We have used THERMIT-UTSG to simulate a SGTR accident in the Calvert Cliffs Nuclear Plant in which only two of the four reactor coolant pumps trip on low primary system pressure. Boundary conditions for this calculation were taken from the results of a TRAC system simulation of the same accident. A steady-state calculation with no rupture flow was performed first to provide a realistic initial condition for the transient simulation. Then, the transient was run for 2400 s of real time. The primary purpose of this work was to provide an independent assessment of the TRAC calculation.

The steady-state results compared favorably with the TRAC calculation on the primary side. For the given power the average primary mass flux and outlet temperature were close to that calculated by TRAC and the actual plant conditions. However, there was substantial disagreement on the secondary side. THERMIT predicted a much lower recirculation ratio and water inventory and more voiding in the evaporator/riser than TRAC. The recirculation ratio in the plant was between that calculated by the two codes. The TRAC water inventory was close to the plant value. We showed that the recirculation ratio, water inventory, and amount of voiding are interrelated. A larger recirculation ratio leads to less voiding and a larger water inventory. So, the disagreement between the codes is thermodynamically consistent.

Two reasons for this disagreement were identified. First, the two codes use different heat transfer correlations. A steady-state calculation using a special version of THERMIT-UTSG that contained the TRAC correlations was used to study the impact of the different heat transfer packages. With adjustment of the tube fouling factor we were

able to obtain a steady-state that matched the primary-side conditions and was closer to the actual plant parameters on the secondary side. The recirculation ratio was close to the plant value. Although the water inventory was still low, use of the TRAC heat transfer correlations significantly improved this quantity.

The second reason for the disagreement between TRAC and THERMIT at steady-state is the different method of phase separation used in the steam dome. In THERMIT all the vapor that leaves the riser will flow out the steam line except for the small amount that condenses. This is also what we expect that occurs in the plant. The TRAC model allows only vapor to flow out the steam line. However, there is no provision to extract most of the vapor from the flow leaving the riser. An examination of the TRAC output showed that a significant amount of vapor is recirculated to the downcomer where it is condensed by the cold feedwater. This problem with phase separation produces more recirculation flow than should exist. Therefore, because of the dependency on the recirculation ratio, there is a higher water inventory and less voiding in TRAC calculation than would occur if the phase separation were correct. The fact that TRAC matched the water inventory of the plant is then probably fortuitous.

To calculate a steady-state that is in good agreement with some standard such as plant data or another calculation, some adjustment in model parameters that are not well known can be made. Such parameters include: U-tube fouling factor, heat transfer areas, additive friction losses. In our heat transfer study we showed that adjustment of the fouling factor primarily affects the primary-side conditions. Changing the heat transfer areas (which numerically is equivalent to changing the

heat transfer coefficients) affects both the primary and secondary-side conditions. A change in the additive friction losses should produce the same result. Further improvement of the THERMIT steady-state can be made by adjusting these parameters. However, care and judgement should be exercised since this may artificially improve the model while masking some deficiency. This could detrimentally affect the transient response of the model.

The THERMIT calculation produced a substantial crossflow between the hot and cold channels, driven by the small pressure difference between the channels. When the axial flow is low compared to the crossflow (low recirculation ratio), the crossflow tends to homogenize the channels, reducing the asymmetry. However, when the axial flow is large compared to the crossflow (such as in the calculation using the TRAC heat transfer correlations) the asymmetry between the channels persists throughout the evaporator/riser.

In the transient calculation the primary system slowly depressurize due to the rupture flow until the reactor scrams on low primary pressure at 928 s after tube rupture. Prior to this, the conditions change very slowly. In a transient calculation THERMIT no longer imposes the reacto power as in steady-state, but instead, uses the primary mass flux. The small difference between the THERMIT and TRAC mass fluxes at steady-stat produces a slight initial divergence of the two calculations.

The rupture flow rate is so small compared to the feedwater flow rate and the riser flow rate that it has only a slight effect on the secondary-side conditions. The rupture flow has the immediate effectof reducing the steam flow and increasing the recirculation flow, since its enthalpy is substantially lower than the highly voided fluid at the top

of the tube bundle. However, the unvaporized rupture flow is recirculated to the downcomer where it has the same effect as a hot feed source. This increases the voiding in the evaporator/riser and hence th outlet steam flow. The net result is a slight reducton in recirculation flow, more steam production, and a small decrease in water inventory. 0 the other hand, the TRAC calculation showed the exact opposite trend -- an increase in recirculation flow and an increase of almost 10,000 kg in water inventory. This is probably the result of the phase separation method mentioned previously. Too much vapor is being recirculated to the downcomer where it is condensed by the feedwater. Hence, the system shows an accumulation of liquid during this period.

Following reactor scram, conditions change rapidly for about 90 s in response to the pressure increase in the secondary side, resulting from turbine trip, the drop in reactor power, and the shutdown of the main feedwater. The heat transfer to the secondary side, steam flow, and secondary-side flows all drop sharply following these events. During this time there is considerable internal circulation within the evaporator/riser with the liquid increasingly falling back as the flow decreases. Conditions change in comparison more slowly after this 90 s period following scram as the flow on the secondary side is very low.

About 30 s after scram the downcomer flow begins to reverse. First, the cold-side downcomer reverses. Then, the hot-side downcomer reverses with flow on the cold-side reversing back to the usual direction. By 70 s after scram the net downcomer flow is negative. This behavior is somewhat questionable since there is no crossflow between the downcomer channels except at the bottom and above the feedwater ring. However, the time interval between the initial reversal

and when the net downcomer flow becomes negative (reversed) is small. Also, the magnitude of the flow is very low -- approaching stagnationn after the feedwater is shut off. There is no flow from the downcomer up into the steam dome. Rather, the reversed flow from the hot-side downcomer flows back down the cold side with a little evaporation in the upper downcomer.

TRAC also predicted downcomer flow reversal, but not until 1190 s (260 s after scram). This is because the TRAC flow, which is higher than in THERMIT at steady-state and prior to scram, falls off relatively slowly after the MFW is off. Beyond 1190 s the flow oscillates, reversing frequently. The magnitude of the oscillations is sometimes substantial. This behavior is questionable and may indicate that the TRAC model is hydrodynamically underdamped. When reversal occurs in TRAC, there is flow from the downcomer into the steam dome and back into the riser. No such behavior was predicted by THERMIT, nor is expected in the actual plant.

Immediately following scram the feedwater flow exceeds the steam flow and there is substantial water accumulation in the system. Even though there is an increase in water inventory, the distribution of the water changes as the boiling front in the evaporator rises. During this time the downcomer water level actually drops. In the long term there is a slow filling of the steam generator due to the rupture flow. Both THERMIT and TRAC predict similar trends in the water inventory although the large difference in water inventory at steady-state persists throughout the transient.

THERMIT predicted a gradual increase in the boiling front over 650 s following scram. The void gradient became progressively steeper

as the upper evaporator boiled dry. There was a little superheating during portions of transient. By 1600 s a sharp interface between the vapor and liquid had formed. However, this interface was well below the location of the break. There is no column of liquid above the break to hydrostatically control the leakage and terminate the accident early as some reports have predicted. A larger initial water inventory may have produced this desired result.

In the TRAC calculation the boiling front remained nearly stationary until 1540 s. Then, a relatively sudden collapsing of the void occurred with the boiling front moving above the tube bundle into the riser. One would expect that a gradual rise in the boiling front at this time in the transient would be more reasonable.

In the TRAC calculation there was essentially no more steam leaving the system through the relief valves after 1590 s. However, since the response of the THERMIT and TRAC models was very different prior to this time, the THERMIT calculation was inconsistent with the supplied boundary conditions. For the steam dome pressure predicted by TRAC, THERMIT calculated a negative steam flow (into the steam generator). Since this is nonphysical we switched to a zero steam flow boundary condition and allowed the code to calculate the steam dome pressure. In response to this change the steam dome pressure dropped substantially. This is an indication of how different the cumulative response of the two models was prior to this time. Such inconsistencies are inevitable when performing component analysis using boundary conditions supplied by a different model -- there is no feedback from the THERMIT steam generator to the rest of the system which is represented by boundary conditions. The problem is further complicated by the fact that a lower

secondary-side pressure should cause an increase in the rupture flow and thus prolong the accident.

In summary the THERMIT and TRAC steam generator models behave very differently. We have pointed out problems with both calculations that require further attention. The differences are substantial enough to indicate that substantial additional investigation and code development are needed to gain more than a basic understanding of steam generator behavior during such accidents and to provide a simulation capability that is acceptable.

References

1. T. F. Bott and E. W. Barts, "Summary of TRAC Analysis of Steam Generator Tube Rupture Calculations for Calvert Cliffs," Technical Letter Report to NRC, Los Alamos National Laboratory, 1985.

2. H. C. da Silva Jr., "Thermohydraulic Analysis of U-Tube Steam Generators," Ph.D. Thesis, Massachusetts Institute of Technology, 1984.

3. J. E. Kelly, "Development of a Two-Fluid, Two-Phase Model for Light Water Reactor Core Analysis," Ph.D. Thesis, Massachusetts Institute of Technology, 1980.

4. J. Loomis, W. H. Reed, A. Schor, H. B. Stewart, L. Wolf, "THERMIT: A Computer Program for Three-Dimensional Thermal-Hydraulic Analysis of Light Water Reactor Cores," EPRI Report, NP-2032, 1981.

5. E. L. Burley, "Performance of Internal Steam Separation Systems in Boiling Water Reactors," ASME 69-WA/NE-24, 1969.

Appendix

Comparison of the THERMIT-UTSG and TRAC Calculations for Case 3

Time (s)	THERMIT-UTSG	TRAC
<0	Full power, steady-state operation	Full power, steady-state operation
0	SGTR	
574	Pressurizer heaters off on low pressurizer level	
0-928.29		*Primary pressure decreasing
	Evaporator/riser void nearly constant	Evaporator/riser void decreases slightly
	Downcomer and riser flows decrease slightly	Downcomer and riser flows increasing
	Downcomer water level and inventory falling slowly	Water inventory increasing
928.29	Reactor trip (scram) on low primary pressure (13.0 MPa)	
	TSV and TBV close; Condenser unavailable	
	MFW Trip: flow coastdown over next 60 s	

*Values of TRAC calculation used for THERMIT-UTSG boundary conditions

Time (s)	THERMIT-UTSG	TRAC
928.29+	ADVs and SRVs open	
928.29-988		*Sharp drop in primary pressure, primary inlet temperature and rupture flow temperature *Rupture flow decreases *Primary mass flux drops slightly *Sharp rise in steam dome pressure *Main feedwater is coasting down
	Sharp drop in heat transfer rate to secondary side	Sharp drop in heat transfer rate to secondary side
	Water level falls to just above the feedwater ring	
	Water inventory increases by ~11,000 kg	Water inventory increase by ~20,000 kg
	Downcomer and riser flows drop to nearly zero	Sharp drop in downcomer and riser flows but still large (~2000 kg/s)
	Sharp drop in steam flow	Sharp drop in steam flow
	Boiling front rises gradually	Boiling front rises slightly and falls
	Axial void gradient increases with liquid drops disappearing in riser	Void fraction decreases throughout the evaporator/riser

Time (s)	THERMIT-UTSG	TRAC
	Increasing liquid fall-back in riser -- primarily droplets in the upper, hot channel	
	Much internal circulation with relatively strong crossflows	
950-960	Flow reversal in the cold-side downcomer	
960-970	Flow reverses back in the cold-side downcomer	
	Flow reverses in the hot-side downcomer	
988	MFW off	
1000	Operator manually sets ADVs open	
1028	SRVs Close	
988-1076		*Primary pressure still falling *Primary-side mass flux and inlet temperature are nearly constant (as well as rupture flow temperature) *Rupture flow still decreasing *Steam dome pressure falling slowly
	S.G. heat transfer rate continues to fall but begins to level out	S.G. heat transfer rate continues to fall but begins to level out

Time (s)	THERMIT-UTSG	TRAC
	Net downcomer and riser flows fall to nearly zero. There is a flow asymmetry in the hot-side and cold-side downcomers with the hot-side downcomer flow reversed.)	Downcomer and riser flows are still high and falling at a slower rate
	Small steam flow (~30 kg/s)	Small steam flow (~40 kg/s)
	Boiling front drops slightly	Boiling front is stationary
	Continuing disappearance of droplets in the riser	Void distribution is nearly constant
1076	2 RCPs tripped on low primary pressure (9.065 MPa). The other two remain on.	
1140	Operator closes MSIV	
1076-1180		*Primary pressure and rupture flow increase slightly
		*Primary mass flux falls sharply to about half its original value
		*Steam dome pressure drops and starts to increase
	Water level and inventory are nearly constant	Water inventory is nearly constant
	Asymmetric downcomer flow; very low riser flow	Downcomer and riser flows drop to nearly zero
	Steam flow slowly decreases to zero	Steam flow slowly decreases to zero
	Two-phase region narrows slightly	Void profile is nearly constant

Time (s)	THERMIT-UTSG	TRAC
	Steam starts to superheat in the riser	Low void in the riser
1190-1200	Asymmetric downcomer flow; very low riser flow	Downcomer and riser flows reverse. Void collapses to only a few percent throughout the evaporator/riser
1200	Operator Closes ADVs	
1220	SRVs open on high steam dome pressure (6.9 MPa)	
1260	Operator closes MFWIV	
1320	Operator closes AFWIV	
1380	Operator verifies damaged S.G. isolation	
1440	Operator turns pressurizer spray on to reduce primary system pressure	
1200-1590		*Primary pressure and rupture flow increase, level off, and start falling *Primary-side temperature decreasing slightly *Steam dome pressure and primary mass flux are nearly constant
	Water level and inventory are slowly rising	Water inventory is nearly constant

Time (s)	THERMIT-UTSG	TRAC
	Asymmetric downcomer flow; very low riser flow	Downcomer and riser flows are oscillating and reversing. There is a big riser flow spike at 1250 s (1670 kg/s)
	Small steam flow	Small steam flow
	Boiling front decreases slightly, remains constant, then increases	Void fraction rises back to nearly its original value (before 1190 s) throughout the evaporator/riser, then begins to fall slowly
	Riser still has pure vapor (superheated)	
1590	SRVs are essentially closed (very low steam flow)	
		Evaporator begins transferring heat to the primary side
1600	Change steam dome pressure boundary condition to no steam flow condition	
1590-1620	Void gradient is very steep steep → sharp vapor-liquid interface	Void collapses in evaporator and lower riser. Boiling front moves to the upper riser.
1620-2400		*Primary pressure and rupture flow falling slowly
		*Primary mass flux rising slowly
		*Primary-side temperature is decreasing

Time (s)	THERMIT-UTSG	TRAC
		*Steam flow is negligible
	Direction of heat transfer reverses ~2140s (secondary to primary)	
	Steam dome pressure falling	Steam dome pressure is constant
	Water level and inventory are increasing (more rapidly after 2200 s)	Water inventory is increasing
	Asymmetric downcomer flow; riser flow is very low	Downcomer and riser flows are oscillating and reversing less→ very low
	Sharp vapor-liquid interface (Short two-phase region)	Sharp vapor-liquid interface but high in the riser
	Riser is no longer superheated	